AECL-6819

ATOMIC ENERGY OF CANADA LIMITED

L'ENERGIE ATOMIQUE DU CANADA LIMITEE

POINT-DEFECT MIGRATION INTO AN INFINITESIMAL DISLOCATION LOOP: EFFECTS OF THE ANISOTROPY OF THE SADDLE-POINT CONFIGURATION

MIGRATION DU DEFAUT DANS UN RESEAU EN BOUCLE DE DISLOCATION INFINITESIMALE: EFFETS DE L'ANISOTROPIE DE LA CONFIGURATION DU DEFAUT

C. H. Woo

Whiteshell Nuclear Research Establishment

Etablissement de Recherches Nucléaires de Whiteshell

Pinawa, Manitoba R0E 1L0

November 1981 novembre

ATOMIC ENERGY OF CANADA LIMITED

POINT-DEFECT MIGRATION INTO AN INFINITESIMAL DISLOCATION LOOP: EFFECTS OF THE ANISOTROPY OF THE SADDLE-POINT CONFIGURATION

by

C.H. Woo

Whiteshell Nuclear Research Establishment
Pinawa, Manitoba ROE 1LO
1981 November

AECL-6819

MIGRATION DU DEFAUT DANS UN RESEAU EN BOUCLE DE DISLOCATION INFINITESIMALE: EFFETS DE L'ANISOTROPIE DE LA CONFIGURATION DU DEFAUT

par

C.H. Woo

RESUME

On décrit la migration du défaut dans un réseau en boucle de dislocation coin infinitésimale d'un milieu élastique linéaire isotropique. On a pris soin tout particulièrement de tenir compte des effets de l'anisotropie de la forme du point de minimum du défaut. Il en découle des expressions des rayons de réaction et d'influence à la fois en la présence et l'absence d'une contrainte externe appliquée. On a constaté qu'ils dépendent de paramètres intrinsèques tels que la résistance de la boucle, la nature de réseau en boucle (inoccuppé ou interstitiel), le volume de relaxation, la forme du point de minimum et les paramètres extrinsèques tels que l'importance et l'orientation de la contrainte externe et la température. On examine les conséquences des résultats.

L'Energie Atomique du Canada Limitée
Etablissement de Recherches Nucléaire de Whiteshell
Pinawa, Manitoba ROE 1LO
1981 novembre

AECL-6819

POINT-DEFECT MIGRATION INTO AN INFINITESIMAL DISLOCATION LOOP: EFFECTS OF THE ANISOTROPY OF THE SADDLE-POINT CONFIGURATION

by

C.H. Woo

ABSTRACT

Point-defect migration into an infinitesimal edge dislocation loop in an isotropic linear elastic medium is described. Particular care has been taken to include the effects of the saddle-point shape anisotropy of the point defect. Expressions for the reaction radii and the bias are derived, both in the presence and absence of an external applied stress. These are found to depend on intrinsic parameters, such as the loop strength, the loop nature (vacancy or interstitial), the relaxation volume, the saddle-point shape, and extrinsic parameters, such as the magnitude and direction of the external stress, and the temperature. The implications of the results are discussed.

Atomic Energy of Canada Limited
Whiteshell Nuclear Research Establishment
Pinawa, Manitoba ROE 1LO
1981 November

AECL-6819

CONTENTS

1. INTRODUCTION

Nuclear reactor structural materials are continuously subjected to the bombardment of energetic particles that produce changes in their lattice structure. This disturbance, in turn, causes changes in the macroscopic material properties, such as dimensional stability, strength and ductility. In most cases, the mechanical properties of the material are adversely affected by the irradiation, from which is derived the phenomenon called irradiation damage.

The potential impact of irradiation damage on the safety and economics of the operation of present fission and future fusion reactors is great. Consequently, considerable world-wide efforts have been expended during the last few decades to gain a comprehensive understanding of the various aspects of irradiation damage, both from the scientific and the engineering points of view.

It is now established[1] that the macroscopic radiation damage effects are the consequences of (i) the continuous production of Frenkel pairs and (ii) the creation of foreign elements, by transmutation, e.g. helium generation by (n,α) reactions. When an energetic particle enters a crystalline solid, it may come into sufficiently close contact with one of the atoms (or nuclei) to impart enough energy to knock it out of its normal lattice site. Depending on the kinetic energy gained by the primary knock-on atom, it may travel further in the crystal and cause displacements of other lattice atoms during its lifetime. The result is a displacement cascade, which can be described as a local 'explosion', where the kinetic energy of the primary knock-on atom is rapidly distributed into the recoil energies of neighbouring lattice atoms. The latter then move out radially until their kinetic energies have decreased to the focusing energy; then replacement collision sequences occur, from which interstitials are created at some distance away from the cascade. This results in a structure made up of a vacancy-rich core surrounded by a halo of interstitials.

The foregoing process takes about 10^{-13} seconds to complete. At the end of this process, the kinetic energy of the atoms is very high, corresponding to about 10^4 K. The probability of spontaneous recombination of the vacancies and interstitials is large. The number of stable defects that survive during the next 10^{-11} seconds, while the cascade cools down, is only a fraction ($\simeq 0.5$) of the number of original displacements.

At reactor operating temperatures, the surviving point defects are free to migrate throughout the crystal, until they

- are annihilated by recombining with point defects of the opposite type,
- are absorbed by crystal defects, such as the dislocation network, dislocation loops, grain boundaries, voids and precipitates,
- combine with impurity atoms, or point defects of the same type, to nucleate point-defect clusters.

The recombination and nucleation events are usually dominant at the beginning of the irradiation, because the sink densities of other crystal defects are low, and annihilation at the crystal-defect sinks is least probable. Under such circumstances, the interstitials form stable (high binding energy), three-dimensional clusters that collapse to interstitial dislocation loops when the number of interstitials exceeds about ten. In contrast to the interstitials, which always agglomerate to planar dislocation loops, different morphologies have been observed in the case of vacancy clusters. Besides dislocation loops, stacking fault tetrahedra and voids are observed, depending on the size and morphology of the displacement cascades and the defect mobility. At this point, we note that an investigation of the stability of small vacancy aggregates[2] has shown that the void morphology is not energetically favourable, compared to planar vacancy clusters. Therefore, in the absence of inhomogeneities, like small gas bubbles or precipitates, one does not expect

vacancies to form three-dimensional clusters, such as voids. From this argument, it is probably not unreasonable to assume that all the displacement cascades collapse to vacancy loops, and voids are nucleated by the free vacancies clustering on inhomogeneities in the lattice.

Vacancies loops, interstitial loops, and voids are three of the most important intrinsic lattice defects nucleated by energetic particle irradiation. Macroscopic effects of irradiation damage, such as void swelling, irradiation creep and growth depend, in detail, on the evolution of these defects (plus others that are present independent of the irradiation, such as grain boundaries, straight dislocations introduced by preirradiation deformation, and some impurities and precipitates). The evolution of these lattice defects is, in general, a function of the net rate of flow of vacancies, or interstitials, to them. Thus, if the situation dictates that there is a net flow of vacancies into the void nuclei, then the voids will grow, and a macroscopic volume increase of the material will be observable. Similarly, if conditions are such that a net flow of interstitials goes to the dislocation loops, the interstitial loops will grow and the vacancy loops will shrink. If the Burgers vectors of the loops are not isotropically distributed, a volume-conserved shape change of the specimen will occur.

In the above examples, the voids and dislocation loops, being the final repository for the point defects, are referred to as sinks. We have seen how a difference in the arrival rates of vacancies and interstitials at the sinks can cause dimensional changes of the specimen. It is now understood that such a difference in point-defect arrival rates can be attributed to the fact that:

- the interaction between the vacancies and the sink is different from that between the interstitials and the sink,

- vacancy supersaturation in the medium is different from interstitial supersaturation.

In the first case, the sink is usually described as having a bias towards one of the two kinds of point defects. The presence of biased sinks usually causes a lowered supersaturation of either the vacancies or the interstitials in the medium (because one of them is annihilated at the biased sink at a faster rate than the other). This is also an important contributing factor to the imbalance of the supersaturations of the two kinds of point defects, resulting in an asymmetry in the flow of vacancies and interstitials to the unbiased sinks.

Physically, the interaction between the point defect and the sink affects the point-defect migration into the sink, by modifying the potential barriers to atomic jumps. In most of the calculations done to date, the effect of the point-defect/sink interaction on the point-defect current is described by the continuum theory of drift-diffusion. Within this approximation, the point-defect drift-diffusion current can be written as

$$\underset{\sim}{j} = -D_o \underset{\sim}{\nabla}\rho + D_o \beta \rho \underset{\sim}{\nabla} E \qquad (1)$$

where D_o is the ideal (i.e. in the absence of the drift field) diffusion coefficient, β is the reciprocal of the product of the Boltzmann constant and the absolute temperature, ρ is the point-defect density and E the drift field (the interaction field between the point defect and the sink). In metals, the main contribution to E comes from the elastic interaction between the strain field of the sink and that of the point defect, which is usually modelled as an isotropic expansion (or contraction) center.

Recently, Dederichs and Schroeder[3] have pointed out that the continuum description given by equation (1) is, in general, inadequate. By adopting a microscopic approach, they showed that, firstly, the effect of the drift field on the point-defect mobility was not accounted for, and secondly, there was no clear indication of whether E referred to the point defect in its equilibrium, or its saddle-point, configuration. They did find that if the saddle-point configuration of the point

defect (or the dipole tensor for elastic interaction) is isotropic, then the form of equation (1) can be retained by replacing D_o with $D = D_o \exp[-\beta(E_s - E_g)]$ and E by E_g, where E_s is the drift field when the point defect is in the saddle-point configuration and E_g the corresponding quantity for the equilibrium position. Note that both E_s and E_g are functions of the point-defect position $\underline{r}$. Then it can be shown that the point-defect flux is determined solely by E_s, and all the previous results can be kept, simply by replacing E with E_s and ρ with $\rho \exp[-\beta(E_s - E_g)]$[4,5].

However, saddle-point configurations of point defects, particularly those of vacancies, are not isotropic in general. This is intuitively evident and has been shown to be true in cubic metals by computer simulation[6,7]. Depending on the extent of the anisotropy of the interacting fields, results obtained by modelling the point defect simply as a center of isotropic expansion (or contraction) could be very much in error and important effects might be concealed. To account for the anisotropy of the point-defect strain field, substantial modifications to the continuum drift-diffusion theory are required, and the resulting solution of the boundary-value problem is mathematically complex. However, such an approach is necessary because it could significantly modify previous conclusions.

We have seen that the dislocation loop is an important crystal defect generated during irradiation and that it can play a dominant role in the dimensional stability of materials. Consequently, its function as a point-defect sink has received a great deal of attention. However, in all of these calculations[8-11], the anisotropy of the saddle-point configuration has been neglected. We hope that, by going through the calculation in detail in the case of an infinitesimal edge dislocation loop (IEDL), something may be learned about the saddle-point shape effect, and its implication for other cases can be estimated.

The purpose of this report is to record, in some detail, the complicated mathematics involved in calculating the point-defect drift-diffusion current into an IEDL, including the point-defect saddle-point shape effect (SAPSE). Two cases will be considered: diffusion in the absence of and in the presence of, an external applied stress. Analytic expressions will be derived for the reaction radii as a function of temperature, sink densities and the point-defect dipole tensor. It will be shown that there is an intrinsic and significant difference between the biases of a vacancy-type IEDL and an interstitial-type IEDL. It will also be shown that the application of an external stress changes the biases to different extents, according to the orientation of the stress with respect to the Burgers vector. This stress-induced change in bias due to SAPSE is compared and contrasted with that due to the inhomogeniety effect (generally referred to as SIPA,, which stands for stress-induced preferred absorption).

2. FORMULATION

We consider point-defect drift-diffusion under the action of an applied strain $\xi_{k\ell}$. According to Dederichs and Schroeder[3], this may be described in terms of the renormalized concentration $W = \rho \exp[\beta E_g]$,, by the Lagrangian

$$L[W] = \int \frac{d^3\underset{\sim}{r}}{V} [\tilde{D}_{ij}(\underset{\sim}{r})\partial_i W(\underset{\sim}{r})\partial_j W(\underset{\sim}{r}) - p(\underset{\sim}{r})W(\underset{\sim}{r})], \qquad (2)$$

where V is the integration volume, ∂_i denotes $\partial/\partial r_i$, $p(\underset{\sim}{r})$ is the production rate and $\tilde{D}_{ij}$ is the renormalized diffusion tensor, given by

$$\tilde{D}_{ij} = \frac{1}{2} \sum_{\hat{\underset{\sim}{h}}} h_i h_j \lambda^{o}_{eff}(\hat{\underset{\sim}{h}}) \exp[\beta \xi_{k\ell} P^{s}_{k\ell}(\hat{\underset{\sim}{h}})]. \qquad (3)$$

Here the summation is over all nearest-neighbour jump directions $\hat{\underset{\sim}{h}}$ *,

* The symbol ^ in $\hat{\underset{\sim}{h}}$ denotes the unit vector in the direction of $\underset{\sim}{h}$. This symbol is used throughout the report with similar meaning.

h_i is the ith component of the nearest-neighbour position vector to which a jump occurs, $P^s_{k\ell}(\hat{h})$ is the elastic dipole-tensor (i.e. the double-force tensor) of the point defect at the saddle point in the jump direction $\hat{h}$ and $\lambda^{o(\hat{h})}_{eff}$ is an effective (averaged over different non-equivalent equilibrium configurations of the point defect) ideal lattice-jump frequency in the $\hat{h}$ direction. Here, as in the rest of the report, we sum over repeated indices. Furthermore, we note that W in equation (2) refers to the total concentration of non-equivalent equilibrium configurations[3] of the same defect. For a cubic defect in a cubic crystal, we can neglect the $\hat{h}$ dependences of $\lambda^{o(\hat{h})}_{eff}$ and the nearest-neighbour jump distance. Then we may write equation (3) as

$$\hat{D}_{ij} = D_o \frac{3}{Z} \sum_{\hat{h}} \hat{h}_i \hat{h}_j \exp[\beta \xi_{k\ell} P^s_{k\ell}(\hat{k})] \qquad (4)$$

where D_o is the ideal diffusion coefficient and Z the co-ordination number. In non-cubic crystals, or non-cubic defects, the same assumption leads to an approximation where the anisotropy of the diffusion tensor, resulting from the anisotropy of the crystal lattice, is averaged out. In this approximation, D_o is replaced by the averaged ideal diffusion coefficient D_o^{eff}, which is effectively what is used in equation (1) in most of the previous calculations[8-11]. This approximation is not expected to cause large errors in normal cases where the anisotropy of lattice diffusion is not very severe. Furthermore, since the present study concentrates on drift-diffusion in the presence of an applied stress, which mainly concerns the exponential term in equation (4), the above approximation should not change, at least, the qualitative picture that evolves.

A further approximation necessary to make this problem tractable is the spherical symmetrization procedure first introduced by Schroeder and Dettmann[5], and used successfully by Woo[11] for dislocation loops. Within this approximation, we use a spherical symmetric ansatz for the renormalized density $W(\underset{\sim}{r}) \approx n_o(r)$. The extremum principle of the Lagrangian then gives the following one-dimensional equation

$$\frac{1}{r^2}\frac{d}{dr}\left[r^2 \tilde{D}_{eff}(r)\frac{dn_o}{dr}\right] + p(r) = 0 \tag{5}$$

where $\tilde{D}_{eff}(r)$ is given by

$$\tilde{D}_{eff}(r) = \int \frac{d\Omega}{4\pi} \hat{r}_i \tilde{D}_{ij} \hat{r}_j . \tag{6}$$

Here $d\Omega$ is an elemental solid angle and $\hat{r}_i$ is the ith component of the unit vector $\hat{\xi}$.

To simplify the notation, we denote $\xi_{k\ell} P^s_{k\ell}(\hat{h})$ in equation (4) by $-E_s(\xi;\hat{h})$. Then equations (4) and (6) imply that

$$\tilde{D}_{eff}(r) = 3D_o^{eff} Z^{-1} \sum_{\hat{h}} \int \frac{d\Omega}{4\pi} (\hat{\xi}\cdot\hat{h})^2 \exp[-\beta E_s(\xi;\hat{h})] \tag{7}$$

$$\simeq 3D_o^{eff} \int \frac{d\Omega_{\hat{h}}}{4\pi} \int \frac{d\Omega}{4\pi} (\hat{\xi}\cdot\hat{h})^2 \exp[-\beta E_s(\xi;\hat{h})] \tag{8}$$

if we assume that the jump directions are isotropic and approximate the summation by an integration. Then if we define

$$\langle f(\xi)\rangle_{\xi} \equiv \int \frac{d\Omega_{\xi}}{4\pi} f(\xi) \tag{9}$$

equation (8) can be written as

$$\tilde{D}_{eff}(r) = 3D_o^{eff} \ll (\hat{\xi}\cdot\hat{h})^2 \exp(-\beta E_s) \gg_{\hat{\xi}} \gg_{\hat{h}} . \tag{10}$$

In the following, we denote $\ll (\hat{\xi}\cdot\hat{h})^2 \exp(-\beta E_s) \gg_{\hat{\xi}} \gg_{\hat{h}}$ by $\langle \exp(-\beta E_s)\rangle$. If we further define $\bar{E}_s(r)$ by

$$\exp(-\beta\bar{E}_s) = 3 \langle \exp(-\beta E_s)\rangle \tag{11}$$

then equation (10) becomes

$$\tilde{D}_{eff}(r) = D_o^{eff} \exp(-\beta \bar{E}_s). \qquad (12)$$

If we denote the reaction radius by R_a, the capture radius of the sink by r_σ and the sink-volume (i.e. the total volume divided by the number of sinks) radius by R, we have the following results:

(A) Constant Boundary Concentration Method

In this method, the sink is surrounded by a spherical reservoir with radius, R, centred at the sink, and maintained at a constant concentration $\bar{C}$. The current into the sink is calculated, and the reaction radius is related to the current. From this method, R_a is given by

$$R_a = \left\{ \int_{r_\sigma}^{R} t^{-2} \exp[\beta \bar{E}_s(t)] \, dt \right\}^{-1} \qquad (13)$$

obtained from equation (28) of Woo[11] by putting $\bar{K}_L = 0$.

(B) Effective Medium Approximation

In this case, the production of point defects is considered, in contrast to (A). Sufficient documentation is found in the literature for this method[12] that it is not necessary to describe it here. Using equation (39) of Woo[11], the reaction radius is given by

$$R_a = \left\{ \int_{r_\sigma}^{R} (t^{-2} - t/R^3) \exp[\beta \bar{E}_s(t)] \, dt \right\}^{-1}. \qquad (14)$$

Note that, firstly, the reaction radii calculated using the effective medium approximation are always larger than those obtained using the constant boundary concentration approximation; and, secondly,

the difference between the two decreases as R increases (or the sink density decreases), so that there is no difference in the limit, when the sinks are very dilute.

With the reaction radius calculated, the rate theory can then be invoked to obtain the microstructure evolution and macroscopic effects. Thus, the problem is reduced to the evaluation of $\bar{E}_s$. As pointed out by Schroeder and Dettmann[5], the integrands in equations (13) and (14) are important only for large values of t, because $\bar{E}_s(t)$ has a large negative value for small values of t, as can be seen from the definition of $\bar{E}_s(r)$ in equation (11). Under such circumstances, as shown in Appendix A, we can write, to a good approximation

$$\beta\bar{E}_s(r) \simeq 3\langle\beta E_s\rangle - \frac{3}{2}\langle\beta^2 E_s^2\rangle + \frac{9}{2}\langle\beta E_s\rangle^2. \qquad (15)$$

Our problem now is reduced to the evaluation of $\langle\beta E_s\rangle$ and $\langle\beta^2 E_s^2\rangle$. This will be covered in the following sections.

3. THE INTERACTION ENERGY (No External Stress)

In this section, we evaluate the interaction energy, $E_s(\underset{\sim}{r};\hat{\underset{\sim}{h}})$, between the point defect and the strain field of an IEDL, in the absence of an external stress. We then show that, in general, E_s is not harmonic unless the saddle-point configuration is isotropic.

According to Kroupa[13], the displacement field at $\underset{\sim}{r}$, of an infinitesimal circular dislocation loop of Burgers vector $\underset{\sim}{b}$ in an isotropic medium, is given by

$$\mu_i = \frac{k_o}{r^3}\left\{(1-2\nu)(A_i b_\alpha r_\alpha + b_i A_\alpha r_\alpha - A_\alpha b_\alpha r_i) + \frac{3b_\alpha r_\alpha A_\beta r_\beta r_i}{r^2}\right\} \qquad (16)$$

where $k_o = -[8\pi(1-\nu)]^{-1}$, ν being the Poisson ratio, and A_i is given by

$$A_i = \delta A \hat{n}_i . \tag{17}$$

Here δA is the area of the loop and $\hat{n}_i$ the ith component of the loop normal. Defining the loop strength tensor $Q_{\alpha\beta}$ by

$$Q_{\alpha\beta} = \frac{1}{2} (A_\alpha b_\beta + A_\beta b_\alpha) \tag{18}$$

equation (16) becomes

$$\mu_i = \frac{k_o}{r^3} \left\{ (2\nu-1)(Q_{\alpha\alpha} r_i - 2Q_{i\alpha} r_\alpha) + \frac{3Q_{\alpha\beta} r_\alpha r_\beta}{r^2} r_i \right\} . \tag{19}$$

From this, the strain field $e_{k\ell}$ of the loop can be evaluated by

$$e_{k\ell} = \frac{1}{2} (\partial_k \mu_\ell + \partial_\ell \mu_k) . \tag{20}$$

We obtain

$$e_{k\ell} = \frac{k_o}{r^3} \left\{ (2\nu-1)(Q_{\alpha\alpha}\delta_{k\ell} - 2Q_{k\ell}) + \frac{3}{r^2} [(1-2\nu)\, Q_{\alpha\alpha} r_k r_\ell + 2\nu(Q_{k\alpha} r_\alpha r_\ell + Q_{\ell\alpha} r_\alpha r_k) + Q_{\alpha\beta} r_\alpha r_\beta \delta_{k\ell}] - \frac{15}{r^4} Q_{\alpha\beta} r_\alpha r_\beta r_k r_\ell \right\} . \tag{21}$$

For an edge loop we may write $Q_{\alpha\beta}$ in terms of the Burgers vector:

$$Q_{\alpha\beta} = Q \hat{b}_\alpha \hat{b}_\beta \tag{22}$$

where

$$Q = \pm \delta A b \begin{cases} + \text{ sign for vacancy loops} \\ - \text{ sign for interstitial loops.} \end{cases}$$

If we expand the point-defect dipole tensor $P^s_{k\ell}$ in terms of its eigenvectors $\hat{e}^{(\sigma)}$ ($\sigma = 1,2,3$), we can write

$$P^s_{k\ell} = P p_\sigma \hat{e}^{(\sigma)}_k \hat{e}^{(\sigma)}_\ell \tag{23}$$

where $P = 1/3\ \mathrm{Tr}P^{s}_{k\ell}$ and p_σ is a normalized eigenvalue, i.e. Pp_σ is the σth eigenvalue. We note that this implies

$$\sum_\sigma p_\sigma = 3. \tag{24}$$

Using equations (21) and (23), the interaction energy $E_s = -P^{s}_{k\ell}e_{k\ell}$ can be evaluated, viz.,

$$E_s = -\frac{k_o PQ}{r^3}\Big\{(2\nu-1)(3-2p_\sigma\hat{b}^2_\sigma) + 3[(1-2\nu)\ p_\sigma\hat{r}^2_\sigma + 4\nu\hat{b}_\alpha\hat{r}_\alpha p_\sigma\hat{b}_\sigma\hat{r}_\sigma + 3\hat{b}_\alpha\hat{b}_\beta\hat{r}_\alpha\hat{r}_\beta] - 15p_\sigma\hat{r}^2_\sigma\hat{b}_\alpha\hat{b}_\beta\hat{r}_\alpha\hat{r}_\beta\Big\} \tag{25}$$

where we have used the coordinate system in which the $\hat{e}^{(\sigma)}_{\ell}$ are basis vectors. If we put

$$P = \kappa\Delta V = \frac{2}{3}\frac{1+\nu}{1-2\nu}\,\mu\,\frac{4\pi}{3}\,r_o^3\ (3\varepsilon) \tag{26}$$

and

$$Q = \pi r_L^2\, b \tag{27}$$

where κ is the bulk compressibility, ΔV is the relaxation volume, μ is the shear modulus, r_o the free defect radius in continuum theory, ε the radial strain as the defect is placed in the elastic medium, and r_L the loop radius, equation (25) reduces in the isotropic limit, i.e. with $p_\sigma = 1$ for all σ, to

$$E_s(p_\sigma=1) = \frac{2}{3}\frac{1+\nu}{1-\nu}\,\mu r_o^3\pi\varepsilon r_L^2 b(1-3\cos^2\theta)/r^3. \tag{28}$$

This is exactly the formula usually used for the point-defect/dislocation-loop interaction (see e.g. Bullough et al[14]) in continuum theory calculations.

In a recent paper, Bullough et al[8] showed that if E_s is harmonic, i.e. $\partial_i\partial_i E_s = 0$, then there is no appreciable difference between the point-defect current into a vacancy and an interstitial loop of the

same size. In the following, it will be shown that the point-defect/loop interaction is not, in general, harmonic. It is harmonic only when the dipole tensor $P_{k\ell}$ is isotropic, i.e. when $p_\sigma = 1$. Using the following formulae in equation (25)

$$\partial_i \hat{r}_j = r^{-1}(\delta_{ij} - \hat{r}_i \hat{r}_j)$$

$$\partial_i r_j = \delta_{ij}$$

$$\partial_i r^n = n r^{n-1} \hat{r}_i$$

$$\partial_i \partial_i r^n = n(n-1)r^{n-2} + n r^{n-2}(\delta_{ii}-1)$$

$$= n(n+1)r^{n-2}$$

we obtain

$$\partial_i \partial_i \left\{ \frac{1}{r^3} (2\nu-1)(3-2p_\sigma \hat{b}_\sigma^2) \right\} = (2\nu-1)(3-2p_\sigma \hat{b}_\sigma^2)\ 6r^{-5} \tag{29a}$$

$$\partial_i \partial_i \left\{ \frac{3}{r^5} [(1-2\nu)p_\sigma r_\sigma^2 + 4\nu p_\sigma \hat{b}_\sigma \hat{b}_\alpha r_\sigma r_\alpha + 3\hat{b}_\alpha \hat{b}_\beta r_\alpha r_\beta \right\}$$

$$= \frac{3}{r^5} [6(1-2\nu) + 8\nu p_\alpha \hat{b}_\alpha^2 + 6] \tag{29b}$$

$$-\partial_i \partial_i \left\{ \frac{15}{r^7} p_\sigma r_\sigma^2 \hat{b}_\alpha \hat{b}_\beta r_\alpha r_\beta \right\}$$

$$= 15 \left\{ \frac{14}{r^9} p_\sigma \hat{b}_\alpha \hat{b}_\beta r_\sigma^2 r_\alpha r_\beta - \frac{1}{r^7} [6\hat{b}_\alpha \hat{b}_\beta r_\alpha r_\beta + 8p_\sigma \hat{b}_\sigma \hat{b}_\beta r_\sigma r_\beta + 2p_\sigma r_\sigma 2] \right\} \tag{29c}$$

and therefore, from equation (25)

$$\partial_i \partial_i E_s = -\frac{k_o PQ}{r^5} (p_\sigma - 1) \left\{ 12\hat{b}_\sigma^2 - 30\hat{r}_\sigma^2 + 15[14\hat{r}_\sigma^2 (\hat{r}_\alpha \hat{b}_\alpha)^2 - 8\hat{b}_\sigma \hat{b}_\beta \hat{r}_\sigma \hat{r}_\beta] \right\}. \tag{30}$$

Equation (30) clearly shows that, unless $p_\sigma = 1$ for all σ, $\partial_i \partial_i E_s$ is non-zero. This result immediately points to the possibility of a difference between the point-defect current into loops of different character (i.e. vacancy or interstitial), thus giving rise to a bias difference between the two. This difference is intrinsic and is entirely a consequence of the anisotropy of the point-defect dipole tensor at the saddle point. In the following, we evaluate the energy $\bar{E}_s$ and the corresponding reaction radius R_a. From this, we will then be able to examine more closely the details, the magnitude and the consequences of this difference.

4. EVALUATION OF $\beta\bar{E}_s$

In the last section, we obtained an expression for $E_s(\hat{\underset{\sim}{h}};\underset{\sim}{r})$, given by equation (25). We are now ready to calculate the averaged saddle-point energy $\beta\bar{E}_s$ according to equation (15),

$$\beta\bar{E}_s = 3\langle\beta E_s\rangle + \frac{9}{2}\langle\beta E_s\rangle^2 - \frac{3}{2}\langle\beta^2 E_s^2\rangle. \tag{15}$$

For simplicity, we assume $\hat{\underset{\sim}{h}} = \hat{\underset{\sim}{e}}^{(1)}$, i.e. the first principal direction of the dipole tensor at the saddle point is along the jump direction. This is not a bad assumption in most cases because $\hat{h}$ is, in general, along a direction of high symmetry of the saddle-point configuration. At any rate, modification of the following analysis to the general case is straightforward.

Evaluation of integrals of the type*

$$\gamma(i_1, i_2 \ldots i_n) = \int \frac{d\Omega}{4\pi} \hat{r}_{i_1} \hat{r}_{i_2} \ldots \hat{r}_{i_n} \tag{31}$$

constitutes the most difficult part of the calculation. These integrals can be expressed as a sum of products of Kronecker delta functions. A

* Note that repeated arguments in γ are not summed over.

general expression for $\gamma(i_1,\ldots i_n)$ would be made up of $n!/2^{n/2}(n/2)!$ terms. In the present case the highest n involved is n=10, corresponding to a total of 945 terms. Fortunately, the presence of repeated indices makes it possible to reduce the number of terms drastically. Induction formulae can then be used to calculate these integrals. A more detailed account of the evaluation of these integrals is given in Appendix B.

4.1 EVALUATION OF $\langle \beta E_s \rangle$

We can derive the following

$$\langle (2\nu-1)(3-2p_\sigma \hat{b}_\sigma^2) \rangle = \frac{1}{3}(2\nu-1)$$

$$\langle 3(1-2\nu)\, p_\sigma \hat{r}_\sigma^2 \rangle = 3(1-2\nu)\, p_\sigma\, \gamma(11\sigma\sigma)$$

$$= \frac{1}{5}(1-2\nu)(3+2p_1)$$

$$\langle 12\nu p_\sigma \hat{b}_\sigma \hat{b}_\alpha \hat{r}_\sigma \hat{r}_\alpha \rangle = \frac{4\nu}{5}\left(1+\frac{2}{3}p_1\right)$$

$$\langle 9\hat{b}_\alpha \hat{b}_\beta \hat{r}_\alpha \hat{r}_\beta \rangle = 1$$

$$\langle 15 p_\sigma \hat{b}_\alpha \hat{b}_\beta \hat{r}_\sigma^2 \hat{r}_\alpha \hat{r}_\beta \rangle = 1 + \frac{2}{3}p_1 .$$

Substituting into equation (25), we obtain

$$\langle \beta E_s \rangle = -\frac{\beta P Q k_o}{r^3}\frac{4}{15}(1+\nu)(1-p_1). \qquad (32)$$

Note that $\langle \beta E_s \rangle$ vanishes when $p_1 = 1$, for the isotropic case. It can be seen from equation (28) that this is the correct limit. We also note that the sign of $\langle \beta E_s \rangle$ depends on the sign of Q and hence on whether the loop is vacancy or interstitial in character (see equation (22)). If for one type of loop $\langle \beta E_s \rangle$ constitutes an attractive contribution to the interaction potential, then it would be a repulsive contribution for the other type. It is $\langle \beta E_s \rangle$ that distinguishes between the magnitude of the

point-defect current into the two types of loops. Such a distinction vanishes with $\langle \beta E_s \rangle$, as the point-defect shape becomes isotropic at the saddle point.

4.2 EVALUATION OF $\langle \beta^2 E_s^2 \rangle$

From equation (25), we can write

$$\beta^2 E_s^2 = \frac{\beta^2 P^2 Q^2 k_o^2}{r^6} \Big\{ (2\nu-1)^2 (3-2p_\sigma \hat{b}_\sigma^2)^2 + 9[(1-2\nu) p_\sigma \hat{r}_\sigma^2 + 4\nu p_\sigma \hat{b}_\sigma \hat{b}_\alpha \hat{r}_\sigma \hat{r}_\alpha$$

$$+ 3(\hat{b}_\alpha \hat{r}_\alpha)^2]^2 + 225(p_\sigma \hat{r}_\sigma^2)^2 (\hat{b}_\alpha \hat{r}_\alpha)^4 + 6(2\nu-1)$$

$$\cdot (3-2p_\sigma \hat{b}_\sigma^2)[(1-2\nu) p_\alpha \hat{r}_\alpha^2 + 4\nu p_\alpha \hat{b}_\alpha \hat{b}_\beta \hat{r}_\alpha \hat{r}_\beta + 3(\hat{b}_\alpha \hat{r}_\alpha)^2]$$

$$- 90 p_\sigma \hat{r}_\sigma^2 (\hat{b}_\alpha \hat{r}_\alpha)^2 [(1-2\nu) p_\sigma \hat{r}_\sigma^2 + 4\nu p_\sigma \hat{b}_\sigma \hat{b}_\alpha \hat{r}_\sigma \hat{r}_\alpha + 3(\hat{b}_\alpha \hat{r}_\alpha)^2]$$

$$- 30 p_\sigma \hat{r}_\sigma^2 (\hat{b}_\alpha \hat{r}_\alpha)^2 (2\nu-1)(3-2p_\sigma \hat{b}_\sigma^2) \Big\}. \qquad (33)$$

$\langle \beta^2 E_s^2 \rangle$ can then be evaluated straightforwardly, term by term. We can derive the following:

$$\langle (2\nu-1)^2 (3-2p_\sigma \hat{b}_\sigma^2)^2 \rangle = \frac{1}{45} (2\nu-1)^2 (8p_\alpha p_\alpha - 9)$$

$$\langle (1-2\nu)^2 p_\alpha p_\beta \hat{r}_\alpha^2 \hat{r}_\beta^2 \rangle = \frac{(1-2\nu)^2}{105} (2p_\alpha p_\alpha + 8p_1^2 + 12p_1 + 9)$$

$$\langle (1-2\nu)(8\nu p_\alpha p_\beta \hat{b}_\beta \hat{b}_\gamma + 6p_\alpha \hat{b}_\beta \hat{b}_\gamma) \hat{r}_\alpha \hat{r}_\alpha \hat{r}_\beta \hat{r}_\gamma \rangle$$

$$= \frac{1-2\nu}{105} \left[\frac{16\nu}{3} p_\alpha p_\alpha + \frac{64\nu}{3} p_1^2 + (32\nu + 28) p_1 + 24\nu + 42\right]$$

$$\langle(16\nu^2 p_\alpha p_\beta + 24\nu p_\alpha + 9)\,\hat{b}_\alpha\hat{b}_\beta\hat{b}_\gamma\hat{b}_\delta\hat{r}_\alpha\hat{r}_\beta\hat{r}_\gamma\hat{r}_\delta\rangle$$

$$= \frac{1}{105}\left(\frac{176\nu^2}{15}\,p_\alpha p_\alpha + 32\nu^2 p_1^{\,2} + \frac{128\nu^2 + 336\nu}{5}\,p_1 + \frac{96\nu^2 + 504\nu + 315}{5}\right)$$

$$\langle p_\alpha p_\beta \hat{b}_i\hat{b}_i\hat{b}_k\hat{b}_\ell\hat{r}_\alpha\hat{r}_\beta\hat{r}_i\hat{r}_j\hat{r}_k\hat{r}_\ell\rangle$$

$$= \frac{1}{10395}\,(38 p_\alpha p_\alpha + 216 p_1^{\,2} + 228 p_1 + 135)$$

$$\langle(2\nu-1)\,(3-2p_\sigma\hat{b}_\sigma^2)[(1-2\nu)\,p_\alpha\hat{r}_\alpha^2 + 4\nu p_\alpha\hat{b}_\alpha\hat{b}_\beta\hat{r}_\alpha\hat{r}_\beta + 3\hat{b}_\alpha\hat{b}_\beta\hat{r}_\alpha\hat{r}_\beta]\rangle$$

$$= \frac{(2\nu-1)}{225}\,[-16\nu p_\alpha p_\alpha - 32\nu p_1^{\,2} + 6(1+2\nu)p_1 + 144 + 18\nu]$$

$$\langle p_\sigma\hat{b}_\alpha\hat{b}_\beta\hat{r}_\sigma^2\hat{r}_\alpha\hat{r}_\beta\,[(1-2\nu)\,p_i\hat{r}_i^2 + 4\nu p_i\hat{b}_i\hat{b}_j\hat{r}_i\hat{r}_j + 3\hat{b}_i\hat{b}_j\hat{r}_i\hat{r}_j]\rangle$$

$$= \frac{1}{945}\,[(1 + \tfrac{2}{5}\nu)\,(6 p_\alpha p_\alpha + 24 p_1^{\,2} + 36 p_1 + 27) + \tfrac{3}{5}\,(189 + 126 p_1)]$$

$$\langle(2\nu-1)\,(3-2p_\sigma\hat{b}_\sigma^2)\,p_\alpha\hat{b}_\beta\hat{b}_\gamma\hat{r}_\alpha^2\hat{r}_\beta\hat{r}_\gamma\rangle$$

$$= \frac{1}{1575}\,(2\nu-1)\,(-8 p_\alpha p_\alpha - 32 p_1^{\,2} + 78 p_1 + 153).$$

Each of these expressions has been checked against the isotropic limit ($p_\sigma = 1$ for all σ), where evaluation of the corresponding expressions is much simpler. From these expressions we can evaluate $\langle\beta^2 E_s^{\,2}\rangle$, viz.,

$$\langle\beta^2 E_s^{\,2}\rangle = \frac{\beta^2 P^2 Q^2 k_o^{\,2}}{r^6}\,[\frac{16}{15}\,(2\nu-1)^2 + C_1(p_\alpha p_\alpha - 3) + C_2(p_1^{\,2}-1) + C_3(p_1-1)] \qquad (34a)$$

where

$$C_1 = \frac{11000\nu^2 - 7568\nu + 7760}{17325}\,, \qquad (34b)$$

$$C_2 = \frac{2112\nu^2 + 4224\nu + 42720}{17325}\,, \tag{34c}$$

$$C_3 = \frac{25344\nu^2 - 82368\nu - 16272}{17325}\,. \tag{34d}$$

For the isotropic case, only the first term in the square brackets in equation (34a) remains. That this is correct can be checked against the isotropic case, using equation (28). Substituting into equation (13), we obtain an expression for $\beta\bar{E}_s$,

$$\beta\bar{E}_s = -\frac{4}{5}(1+\nu)(1-p_1)\frac{\beta PQk_o}{r^3} - \left\{\frac{8}{5}(1-2\nu)^2 + \frac{3}{2}C_1(p_\alpha p_\alpha - 3) + \frac{3}{2}C_2(p_1^2-1) + \frac{3}{2}C_3(p_1-1) - \frac{8}{25}(1+\nu)^2(1-p_1)^2\right\}\frac{\beta^2P^2Q^2k_o^2}{r^6}\,. \tag{35}$$

If we make the transformation

$$t = |\beta PQk_o|^{-1/3}\, r \tag{36}$$

equation (35) becomes

$$\beta\bar{E}_s(t) = At^{-3} - Bt^{-6} \tag{37}$$

where

$$A = \frac{4}{5}(1+\nu)(1-p_1)\,\text{sign}\,(PQ) \tag{38a}$$

$$B = 1.6(1-2\nu)^2 + 1.5C_1(p_\alpha p_\alpha - 3) + 1.5C_2(p_1^2-1) + 1.5C_3(p_1-1) - 0.32(1+\nu)^2(1-p_1)^2 \tag{38b}$$

and $\text{sign}\,(f) = \begin{cases} +1 \text{ for } f > 0 \\ -1 \text{ for } f < 0. \end{cases}$

Note that A vanishes, and only the first term of B survives, when the point defect has an isotropic configuration at the saddle point. It is very satisfying to find that equation (37) indeed reduces to the isotropic limit, which can be easily calculated starting with equation (28).

5. THE REACTION RADIUS AND BIAS (No External Stress)

In this section, we use the expression for $\beta\bar{E}_s$ derived in equation (37) to calculate the reaction radius, using equations (13) and (14). An expression for the bias of an edge dislocation loop is then derived. We then calculate explicitly the difference between the biases of a vacancy loop and an interstitial loop.

Substitution of equation (37) into equation (13) yields, for the reaction radius for the constant-boundary concentration method:

$$R_a = |k_o \beta PQ|^{1/3} \left[\int_{t_\sigma}^{t_R} t^{-2} \exp(At^{-3} - Bt^{-6})dt\right]^{-1} \qquad (39)$$

where

$$t_\sigma = |k_o \beta QP|^{-1/3} r_\sigma, \qquad (40a)$$

$$t_R = |k_o \beta QP|^{-1/3} R. \qquad (40b)$$

Similarly, for the effective medium approximation, we have from equation (15),

$$R_a = |k_o \beta PQ|^{1/3} \left[\int_{t_\sigma}^{t_R} (t^{-2} - tR^{-3}) \exp(At^{-3} - Bt^{-6})dt\right]^{-1}. \qquad (41)$$

In the limit of low sink density, i.e. $R \to \infty$, expressions (39) and (41) become equal. For simplicity, we only attend to this case in the following discussion. We believe the conclusions also apply for finite R values.

Before proceeding, let us consider the choice of the capture radius, r_σ, which defines a spherical surface on which the thermal equilibrium boundary condition is to be supplied, and which encloses a region where the point defect can be considered to be captured by the sink. In other words, it is a region from which a newly arrived point defect will find it difficult to leave by thermal motion alone. It can only be annihilated at the sink. Outside this region, drift-diffusion takes place. In this regard, we follow Schroeder and Dettmann[5] and choose the capture region to be one bounded by the surface on which $E_g(\infty) - E_g(\underset{\sim}{r}) \approx \beta^{-1}$. However, such a region is not spherically symmetric and it is difficult to specify a capture radius. Fortunately, since the drift field ensures that most of the point-defect current enters the sink on the negative side of the drift potential, we may define the capture radius by requiring it to satisfy

$$E_g(\infty) - \min E_g(r_\sigma) = \beta^{-1}. \tag{42}$$

This definition may overestimate r_σ. Nevertheless, we shall see that the reaction radius calculated according to equations (39) and (41) is not very sensitive to this overestimation, because the integrand is small for small values of t.

The drift field at the equilibrium configuration can be derived in the same way as equation (25) and would have the same form, with P replaced by P_g, and p_σ by p_σ^g. The minimum occurs at $\hat{\underset{\sim}{r}} = \hat{\underset{\sim}{b}}$, or $\hat{\underset{\sim}{r}} \cdot \hat{\underset{\sim}{b}} = 0$, depending on the sign of $k_o PQ$. In the first case ($\hat{\underset{\sim}{r}} = \hat{\underset{\sim}{b}}$; $k_o PQ > 0$)

$$\beta E_g\Big|_{\hat{\underset{\sim}{r}} = \hat{\underset{\sim}{b}}} = -\frac{\beta P_g Q k_o}{r^3}\Big\{(2\nu-1)\ (3-2p_\sigma \hat{b}_\sigma^2) + 3[(1-2\nu)p_\sigma \hat{b}_\sigma^2 + 4\nu p_\sigma \hat{b}_\sigma^2 + 3] - 15 p_\sigma \hat{b}_\sigma^2\Big\} \tag{43}$$

so that

$$\langle \beta E_g \rangle_{\hat{h}} = \frac{k_o \beta P_g Q}{r^3} 4(1-2\nu). \tag{44}$$

Since $E_g(\infty) = 0$, equation (42) then gives

$$[\beta P_g Q k_o \, 4(1-2\nu)]^{1/3} = r_\sigma \tag{45}$$

or

$$t_\sigma = [4(1-2\nu)\left|\frac{P_g}{P}\right|]^{1/3}. \tag{46}$$

For the $\hat{r} \cdot \hat{b} = 0$ case ($k_o P_g Q < 0$),

$$\beta E_g\Big|_{\hat{r} \cdot \hat{b} = o} = \frac{\beta P_g Q k_o}{r^3} \left\{(2\nu-1)\ (3-2p_\sigma \hat{b}_\sigma^2) + 3(1-2\nu)p_\sigma \hat{b}_\sigma^2\right\} \tag{46}$$

resulting in

$$t_\sigma = [2(1-2\nu)\left|\frac{P_g}{P}\right|]^{1/3}. \tag{47}$$

The two results differ by $\sim$ 25%, to which the value of R_a is insensitive (see Figure 1). It is a reasonable approximation to assume

$$t_\sigma \simeq |P_g/P|^{1/3} \simeq 1 \tag{48}$$

for most practical purposes. Thus, in the limit of low sink density, we may write

$$R_a = |k_o \beta P Q|^{1/3} \, S^{-1}(A,B) \tag{49}$$

where S(A,B) is defined by

$$S(A,B) = \int_1^\infty t^{-2} \exp(At^{-3} - Bt^{-6}) dt. \tag{50}$$

We can now calculate the bias B_{jL} of an IEDL:

$$B_{jL} = 1 - \frac{R_a^v}{R_a^i} \tag{51}$$

where j = i for interstitial loops and v for vacancy loops, and the superscript on R_a denotes the type of point defect under consideration, i.e. i for interstitials and v for vacancies. From equation (49) we obtain for vacancy loops

$$B_{vL} = 1 - \left|\frac{P_v}{P_i}\right|^{1/3} \frac{S(A_i^{vL}, B_i)}{S(A_v^{vL}, B_v)} , \tag{52}$$

and for interstitial loops

$$B_{iL} = 1 - \left|\frac{P_v}{P_i}\right|^{1/3} \frac{S(A_i^{iL}, B_i)}{S(A_v^{iL}, B_v)} . \tag{53}$$

The difference between the bias of a vacancy and an interstitial loop lies only in the difference between the A values. As can be seen from equations (38a) and (38b), we always have

$$A_j^{iL} = - A_j^{vL} \quad \text{and} \quad j = i,v \tag{54}$$

because $Q^{iL} = - Q^{vL}$.

Thus, for vacancy and interstitial loops to have the same bias, we must have $A_j^{iL} = 0 = A_j^{vL}$, for both vacancies and interstitials. From equation (38a), this can only happen if both types of point defects have isotropic configurations at the saddle point.

When the saddle-point configuration is anisotropic, we would expect a difference between B_{iL} and B_{vL}. In fact, we can write the difference $B_{iL} - B_{vL} \equiv \Delta B$ as

$$\Delta B = \left|\frac{P_v}{P_i}\right|^{1/3} \left[\frac{S(A_i^{vL},B_i)}{S(A_v^{vL},B_v)} - \frac{S(-A_i^{vL},B_i)}{S(-A_v^{vL},B_i)}\right] \tag{55}$$

where A_j^{vL} is given by equation (38a) as

$$A_j^{vL} = \frac{4}{5}(1+\nu)(1-p_1^j)\ \text{sign}\ (P_j) \tag{56}$$

where the superscript j denotes the type of defect: vacancy (j = v) or interstitial (j = i). We note that S(A,B) - S(-A,B) has the same sign as A. Thus, from equation (55), it can be seen that ΔB has the same sign as A_i^{vL} if $A_v^{vL} = 0$, or if A_i^{vL} and A_v^{vL} have opposite signs. On the other hand, ΔB has the opposite sign to A_v^{vL} if $A_i^{vL} = 0$. In the general case, when both A_v^{vL} and A_i^{vL} are non-zero, and have the same sign, the sign of ΔB then depends on the relative magnitudes of A_i^{vL} and A_v^{vL}. From this discussion, we see that vacancy loops and interstitial loops do have different biases, even if their loop radii are the same[8,11]. This difference originates from the anisotropy of the saddle-point configuration; its sign and magnitude depend on the shape and the degree of distortion of the saddle-point configuration. All this information is contained in A_j^{vL}, which can be rewritten as

$$A^{vL} = \frac{4}{5}(1+\nu)\frac{P_2 + P_3 - 2P_1}{|TrP|}\ . \tag{57}$$

A^{vL} is negative for a defect elongated in the jump direction (cigar-shaped), and positive for one which is flattened in the jump direction (plate-shaped). The opposite is true for A^{iL}. The foregoing discussion can then be easily represented by the following picture. We divide point defects into three types: the cigar-shaped ones being M, the plate-shaped ones being F and the isotropic ones being N. The point-defect shape effect can then be described as follows: relative to N-type defects, vacancy loops are more attractive to M-type defects, and less attractive to F-type defects, and vice versa for interstitial loops. Thus, for example, if the vacancy is an F-type defect and the interstitial an M-type defect, the vacancy loop will have a higher bias (towards

interstitials) than the interstitial loop. Or, if both the vacancy and the interstitial are of the same type, say F, and if the anisotropy of the interstitial is larger than that of the vacancy, then the vacancy loop will have a lower bias than the interstitial loop. Thus, the difference in the biases of the two types of loops is completely governed by the anisotropy of the shape of the point defects at the saddle point. In fact, as can be seen from equations (52) and (53), the bias B is a function of the size factor, $|P_i/P_v|^{1/3}$, as well as the shape factor, $S(A_i,B_i)/S(A_v,B_v)$. It is commonly believed that, since interstitials have a larger relaxation volume than vacancies, dislocation loops would always have a bias towards interstitials; whether it is a vacancy loop or an interstitial loop is immaterial (i.e. $B_{jL} > 0_{\text{for } j = i,v}$). Such reasoning is not necessarily valid when the shape factor is taken into account. The condition for $B > 0$, as derived from equations (52) and (53), is that

$$\frac{S(A_i,B_i)}{S(A_v,B_v)} < \left|\frac{P_i}{P_v}\right|^{1/3} . \tag{58}$$

If $|P_i/P_v|$ is large (say > 10), then equation (58) is likely to be satisfied for both vacancy and interstitial loops. However, if $|P_i/P_v|$ is not so large (say < 3), then, depending on the shape anisotropy, equation (58) may not be satisfied and it is possible to find either the vacancy loop or the interstitial loop to have a bias towards vacancies.

The physical reason for the intrinsically different biases for a vacancy loop and an interstitial loop, when the migrating point defect has an anisotropic shape at the saddle point, is clear from Figures 2 and 3. In Figure 2, we show the flow lines of point defects with a positive relaxation volume (P > o) to a vacancy loop. Also shown is the anisotropic strain field (e_{kl}) of the loop in the region where the point defect enters the loop. It can be seen that e_{kl} is dilated more in the $\hat{b}$ direction than in the other directions. Consequently, an M-type defect would encounter a lower saddle-point energy barrier during its jump along the flow line (the most favoured jump), compared to an isotropic

defect of the same relaxation volume. The opposite is true, of course, for an F-type defect. The case of an interstitial loop is shown in Figure 3. We note that, although the direction of the flow line is changed from along the $\hat{b}$ direction to perpendicular to the $\hat{b}$ direction, the loop strain field is still more dilated along the $\hat{b}$ direction. Thus, F-type defects, with larger dilation perpendicular to the jump direction, would migrate faster than M-type defects with the same relaxation volume, which is opposite to the case for vacancy loops. The case for defects with negative relaxation volume ($P < 0$) can be similarly explained.

The foregoing discussion has a very significant implication for the rate theory description of irradiation damage effects in crystalline materials. Accordingly, materials can be divided into three classes.

The first class contains materials in which both vacancy and interstitial loops have a bias towards interstitials, i.e. $B_{iL} > 0$ and $B_{vL} > 0$. These materials have a large P_i/P_v ratio. When irradiated by either MeV electrons or fast neutrons, void growth will occur. Free vacancy loops (i.e. free from the stress fields of other crystal defects) should not be observed. Examples of this class of materials may be copper, nickel, platinum, silver, gold, iron, vanadium, niobium, molybdenum, tantalum, magnesium and rhenium[15], where void swelling occurs.

The second class contains materials in which interstitial loops have a bias towards interstitials and vacancy loops have a bias towards vacancies, i.e. $B_{iL} > 0$ and $B_{vL} < 0$. These materials have a small P_i/P_v ratio and interstitials are more plate-like at the saddle point than vacancies. Void growth can only occur under MeV-electron irradiation, where vacancy loops are not nucleated (from cascade collapse). Under fast-neutron irradiation, where vacancy loops are created, the vacancy loops will grow instead of voids because the former have a bias towards vacancies, while the latter have no bias. Examples of this class may be zirconium[15,16] and titanium[15].

The third class contains materials in which vacancy loops have a bias towards interstitials and interstitial loops have a bias towards vacancies. These materials also have a small P_i/P_v ratio, but vacancies are more plate-like than the interstitials. Void growth does not occur under MeV-electron or fast-neutron irradiation if straight edge dislocations due to pre-irradiation deformation are absent. Dislocation loops will not be seen because they cannot grow. Examples of this class of materials have not been observed. However, with the small number of elements or alloys on which irradiation experiments have been performed, not much can be said about this class, except that, if examples exist, they may be useful nuclear structural materials.

Although the foregoing picture of the classification of materials may seem oversimplified, in that there is no account of the influence of impurities, interactions of neighbouring defects, surface effects, stacking faults, dose rates and many other possible factors, it does provide a rough picture that is consistent with our present knowledge of void growth and dislocation-loop growth in irradiated materials. Before ending this section, one must emphasize that the above discussion applies only to the irradiation situation where a supersaturation of vacancies and interstitials is continuously being maintained. In this case, the difference in point-defect arrival rates at the dislocation loops, due to a difference in the drift currents, is maintained during the irradiation and causes profound microstructural effects. Such subtle drift-field effects are generally not important in processes which occur at point-defect concentrations close to their thermal equilibrium values.

6. THE EFFECTS OF AN EXTERNALLY APPLIED STRESS

The effect of an externally applied stress on the bias of a straight dislocation was first considered by Heald and Speight[17] and

Wolfer and Ashkin[18]. It was envisaged to be caused by a change in the point-defect/dislocation interaction due to the induced change in the dipole tensor by an external shear. This is the basis of the SIPA mechanism often used to explain the phenomenon of irradiation creep[17-21]. In a recent article, it was suggested by Savino[22], and supported by Dederichs and Schroeder[3], that the non-equivalence of the jump directions in external fields due to the anisotropy of the saddle-point configurations could add to the effect on the bias. However, because of the complexity of the mathematics, the significance of this contribution has not been evaluated. Using the formulation and results developed in the foregoing sections, we can perform the calculation for an IEDL.

Suppose the material is acted on by a uniform external applied stress causing a strain field $\varepsilon_{k\ell}$ given by

$$\varepsilon_{k\ell} = \varepsilon s_\alpha \hat{t}_k^{(\alpha)} \hat{t}_\ell^{(\alpha)} \tag{59}$$

where $\hat{t}^{(\alpha)}$ is the unit vector of the αth principal direction, εs_α is the αth eigenvalue and ε is given by $\mathrm{Tr}(\varepsilon_{k\ell})/3$, so that s_α is normalized by $\sum_\alpha s_\alpha = 3$. The total strain field $\xi_{k\ell}$ (external + IEDL) on the point defect is given by

$$\xi_{k\ell} = \varepsilon_{k\ell} + e_{k\ell} \tag{60}$$

where $e_{k\ell}$ is the strain field due to the IEDL in equation (21). The interaction energy $E_s(\underset{\sim}{r};\hat{h})$ is then given by

$$E_s(\underset{\sim}{r};\hat{h}) = - e_{k\ell} P_{k\ell} - \varepsilon_{k\ell} P_{k\ell} \tag{61}$$

where the first term is given by equation (25) and the second term by

$$\varepsilon_{k\ell} P_{k\ell} = \varepsilon P p_\sigma s_\alpha \hat{e}_\alpha^{(\sigma)} \hat{e}_\alpha^{(\sigma)}. \tag{62}$$

Here we have chosen the co-ordinate system in which the $\hat{\underset{\sim}{t}}^{(\alpha)}$ values are the basis vectors.

The change of the reaction radius, ΔR_a, of the IEDL due to $\epsilon_{k\ell}$, is given by

$$\Delta R_a = \left.\frac{dR_a}{d\epsilon}\right|_{\epsilon=0} \epsilon. \tag{63}$$

Substitution into equations (13) and (14) gives, for the constant boundary concentration model,

$$\frac{\Delta R_a}{R_a} = -\epsilon \frac{\int_{t_\sigma}^{t_R} t^{-2} \left[\exp(\beta\bar{E}_s) \frac{d\beta\bar{E}_s}{d\epsilon}\right]_{\epsilon=0} dt}{\int_{t_\sigma}^{t_R} t^{-2} \left[\exp(\beta\bar{E}_s)\right]_{\epsilon=0} dt} \tag{64}$$

and for the effective medium model,

$$\frac{\Delta R_a}{R_a} = -\epsilon \frac{\int_{t_\sigma}^{t_R} (t^{-2} - R^{-3}t) \left[\exp(\beta\bar{E}_s) \frac{d\beta\bar{E}_s}{d\epsilon}\right]_{\epsilon=0} dt}{\int_{t_\sigma}^{t_R} (t^{-2} - R^{-3}t) \left[\exp(\beta\bar{E}_s)\right]_{\epsilon=0} dt}. \tag{65}$$

As in the case of no external stress, in the following we only consider the constant boundary concentration model, for simplicity.

The change of the bias due to the externally applied stress is, from equation (51)

$$\Delta B_{jL} = \frac{R_a^v}{R_a^i} \left(\frac{\Delta R_a^i}{R_a^i} - \frac{\Delta R_a^v}{R_a^v} \right) \qquad j = i,v. \tag{66}$$

ΔB_{jL} can be calculated from $\Delta R_a/R_a$ when $d\beta\bar{E}_s/d\epsilon$ is known.

In the following, we consider the calculation of $d(\beta\bar{E}_s)/d\varepsilon$.

In the presence of an externally applied uniform stress, $E_s(\underset{\sim}{r})$ in equation (61) can be written as

$$E_s(\underset{\sim}{r}) = E_s^{\,e} + E_s^{\,i}(\underset{\sim}{r}) \tag{67}$$

where $E_s^{\,e}$ $(= -\varepsilon_{k\ell}P_{k\ell})$ is the contribution from the external stress, which is independent of $\underset{\sim}{r}$, and $E_s^{\,i}(\underset{\sim}{r})$ $(= -e_{k\ell}P_{k\ell})$ is the contribution from the internal stress due to the strain field of the loop. To obtain an expression for $\bar{E}_s$ accurate to first order in $E_s^{\,e}$, and second order in $E_s^{\,i}(\underset{\sim}{r})$, we need an expansion of $\langle \exp(-\beta E_s)\rangle$ to third order in $E_s(\underset{\sim}{r})$. Similar to the treatment in Appendix A, we can show that, to this accuracy, E_s can be written as

$$\begin{aligned}\bar{E}_s = {} & 3\langle E_s^{\,i}\rangle - \frac{3}{2}\langle (E_s^{\,i})^2\rangle + \frac{9}{2}\langle E_s^{\,i}\rangle^2 \\ & + 3\langle E_s^{\,e}\rangle\left[1 + 3\langle E_s^{\,i}\rangle - \frac{3}{2}\langle (E_s^{\,i})^2\rangle + 9\langle E_s^{\,i}\rangle^2\right] \\ & + \frac{3}{2}\langle E_s^{\,e}(E_s^{\,i})^2\rangle - 3\langle E_s^{\,e}E_s^{\,i}\rangle\,(1 + 3\langle E_s^{\,i}\rangle).\end{aligned} \tag{68}$$

Terms in the first line do not contribute to $d(\beta\bar{E}_s)/d\varepsilon$ and terms in the second line are independent of the stress direction, because $\langle E_s^{\,e}\rangle = -\langle \varepsilon_{k\ell}P_{k\ell}\rangle = \varepsilon P$. Only terms in the third line are of interest to us because these cause $\bar{E}_s$, and hence B, to vary with the stress direction. This gives rise to a stress-induced preferred absorption effect.

In the following, we evaluate $\langle E_s^{\,e}E_s^{\,i}\rangle$ and $\langle E_s^{\,e}(E_s^{\,i})^2\rangle$.

6.1 EVALUATION OF $\langle E_s^{\,e}E_s^{\,i}\rangle$

$$E_s^{\,e}E_s^{\,i} = e_{k\ell}\varepsilon_{mn}P_{k\ell}P_{mn}. \tag{69}$$

By definition

$$\langle e_{k\ell}\varepsilon_{mn}P_{k\ell}P_{mn}\rangle = \langle\langle e_{k\ell}P_{k\ell}(\hat{r}\cdot\hat{h})^2\rangle_{\hat{r}}\ \varepsilon_{mn}P_{mn}\rangle_{\hat{h}} \tag{70}$$

because ε_{mn} is uniform in space. The average over $\hat{r}$ can be carried out as before:

$$\langle e_{k\ell}P_{k\ell}(\hat{r}\cdot\hat{h})^2\rangle_{\hat{r}} = \frac{k_o PQ}{r^3}\{\frac{4}{15}(1-2\nu)\ [1 - 3(\hat{e}_\alpha^{(1)}\hat{b}_\alpha)^2] + \frac{4}{15}(1+\nu)\ (1-p_1)$$
$$+ \frac{40-56\nu}{105}(p_\sigma-1)\ (\hat{e}_\alpha^{(\sigma)}\hat{b}_\alpha)^2\}. \tag{71}$$

We then have, from equation (70)

$$\langle e_{k\ell}P_{k\ell}\varepsilon_{mn}P_{mn}\rangle = \frac{k_o\varepsilon P^2 Q}{r^3}(T_1 + T_2 + T_3) \tag{72}$$

where

$$T_1 = \frac{4}{15}(1-2\nu)\ \langle[1 - 3(\hat{e}_\alpha^{(1)}\hat{b}_\alpha)^2]\ p_\sigma s_\gamma \hat{e}_\gamma^{(\sigma)}\hat{e}_\gamma^{(\sigma)}\rangle_{\hat{h}}, \tag{73a}$$

$$T_2 = \frac{4}{15}(1-\nu)\ (1-p_1)\ p_\sigma s_\alpha \langle\hat{e}_\alpha^{(\sigma)}\hat{e}_\alpha^{(\sigma)}\rangle_{\hat{h}}, \tag{73b}$$

$$T_3 = \frac{40-56\nu}{105}(p_\sigma-1)\ \hat{b}_\alpha\hat{b}_\beta p_\rho s_\gamma \langle\hat{e}_\alpha^{(\sigma)}\hat{e}_\beta^{(\sigma)}\hat{e}_\gamma^{(\rho)}\hat{e}_\gamma^{(\rho)}\rangle_{\hat{h}}. \tag{73c}$$

Evaluation of the T_i values requires relating $\hat{e}^{(\sigma)}$ to $\hat{h}$ (i.e. $\hat{e}^{(1)}$). In Appendix C we prove the following:

$$\hat{e}_\gamma^{(\sigma)}\hat{e}_\gamma^{(\sigma)}\ \text{(no implied summation)} = \frac{1}{2}\hat{e}_\gamma^{(1)}\hat{e}_\gamma^{(1)}\ (3\delta_{\sigma 1} - 1)$$
$$+ \frac{1}{2}(\delta_{\sigma 2} + \delta_{\sigma 3}). \tag{74}$$

Using equation (75) in equations (74a-74c) we obtain

$$T_1 = \frac{4}{25}\,(1-2\nu)\,(1-p_1)\,(s_\alpha \hat{b}_\alpha^2 - 1), \tag{75a}$$

$$T_2 = \frac{4}{5}\,(1+\nu)\,(1-p_1), \tag{75b}$$

$$T_3 = \frac{40-56\nu}{350}\,(1-p_1)^2\,(s_\alpha \hat{b}_\alpha^2 - 1). \tag{75c}$$

These results have been checked against the case of a uniaxial tensile stress operating parallel to $\hat{k}$ ($s_\alpha \hat{b}_\alpha^2 = 3$). We can therefore write

$$\langle E_s^{\,e} E_s^{\,i} \rangle = \frac{k_o \epsilon P^2 Q}{r^3}\,(1-p_1) \cdot \{\frac{4}{5}\,(1+\nu) + [\frac{4}{25}\,(1-2\nu) + \frac{20-28\nu}{175}\,(1-p_1)]\,(s_\alpha \hat{b}_\alpha^2 - 1)\}. \tag{76}$$

We note that for a pure hydrostatic applied stress, i.e. $s_\alpha = 1$

$$\langle E_s^{\,e} E_s^{\,i} \rangle\Big|_{s_\alpha} = \epsilon P \frac{k_o PQ}{r^3}\,(1-p_1)\,\frac{4}{5}\,(1+\nu) = 3\,\langle E_s^{\,e} \rangle \langle E_s^{\,i} \rangle \tag{77}$$

from equations (32) and (62). This verifies that equation (76) has the correct limit.

6.2 EVALUATION OF $\langle E_s^{\,e} (E_s^{\,i})^2 \rangle$

$$E_s^{\,e} (E_s^{\,i})^2 = e_{ij} e_{k\ell} \epsilon_{mn} P_{ij} P_{k\ell} P_{mn}. \tag{78}$$

By definition

$$\langle E_s^{\,e} (E_s^{\,i})^2 \rangle = - \langle\langle e_{ij} e_{k\ell} P_{ij} P_{k\ell} \rangle_{\hat{k}}\, \epsilon_{mn} P_{mn} \rangle_{\hat{h}}. \tag{79}$$

The average over ξ can be carried out as before, viz.,

$$\langle e_{ij}e_{k\ell}P_{ij}P_{k\ell}\rangle_{\xi} = \frac{k_o^2P^2Q^2}{r^6}(T_1 + T_2 + T_3 + T_4 + T_5 + T_6) \qquad (80)$$

where

$$T_1 = \frac{1}{3}(2\nu-1)^2(3-2p_\alpha\hat{b}_\alpha^2)^2,$$

$$T_2 = \frac{3}{35}\Big\{(1-2\nu)^2(2p_\alpha p_\alpha + 8p_1^2 + 12p_1 + 9)$$
$$+ (1-2\nu)[8\nu(3p_\alpha\hat{b}_\alpha^2 + 2p_1p_\alpha\hat{b}_\alpha^2 + 6p_1\hat{b}_1^2 + 2p_\alpha^2\hat{b}_\alpha^2 + 8p_1^2\hat{b}_1^2)$$
$$+ 6(3 + 2p_1 + 6\hat{b}_1^2 + 2p_\alpha\hat{b}_\alpha^2 + 8p_1\hat{b}_1^2)]$$
$$+ 16\nu^2(p_\alpha^2\hat{b}_\alpha^2 + 2p_1^2\hat{b}_1^2 + 2p_\alpha^2\hat{b}_\alpha^2\hat{b}_1^2 + 2p_\alpha p_\beta\hat{b}_\alpha^2\hat{b}_\beta^2 + 8p_1p_\alpha\hat{b}_1^2\hat{b}_\alpha^2)$$
$$+ 24\nu(3p_\alpha\hat{b}_\alpha^2 + 6p_1\hat{b}_1^2 + 6p_\alpha\hat{b}_\alpha^2\hat{b}_1^2) + 9(3 + 12\hat{b}_1^2)\Big\},$$

$$T_3 = \frac{5}{77}\Big\{(2p_\alpha p_\alpha + 8p_1^2 + 12p_1 + 9) + (36 + 144p_1 + 8p_\alpha p_\alpha + 192p_1^2)\hat{b}_1^2$$
$$+ (24p_\alpha + 24p_\alpha^2 + 16p_1p_\alpha)\hat{b}_\alpha^2\Big\},$$

$$T_4 = \frac{6}{15}(2\nu-1)(3-2p_\alpha\hat{b}_\alpha^2)\Big\{(1-2\nu)(3+2p_1) + 4\nu(p_\beta\hat{b}_\beta^2 + 2p_1\hat{b}_1^2) + 3(1+2\hat{b}_1^2)\Big\},$$

$$T_5 = -\frac{2}{21}\Big\{(1-2\nu)[9 + 12p_1 + 2p_\alpha p_\alpha + 8p_1^2 + (12p_\alpha + 8p_\alpha p_\alpha + 8p_\alpha^2)\hat{b}_\alpha^2$$
$$+ (18 + 4p_\alpha p_\alpha + 48p_1 + 48p_1^2)\hat{b}_1^2]$$
$$+ 12\nu[(3p_\alpha + 2p_1p_\alpha + 2p_\alpha^2)\hat{b}_\alpha^2 + (8p_1 + 6p_1^2)\hat{b}_1^2 + 2p_\alpha p_\beta\hat{b}_\alpha^2\hat{b}_\beta^2$$
$$+ (6p_\alpha + 12p_1p_\alpha + 4p_\alpha^2)\hat{b}_1^2\hat{b}_\alpha^2]$$
$$+ 9[3 + 2p_1 + 4p_\alpha\hat{b}_\alpha^2 + (12 + 16p_1)\hat{b}_1^2 + 8p_\alpha\hat{b}_1^2\hat{b}_\alpha^2]\Big\},$$

$$T_6 = \frac{2}{7}(1-2\nu)[9 + 6p_1 + (18 + 24p_1)\hat{b}_1^2 - 4p_1 p_\alpha \hat{b}_\alpha^2 - (12 + 16p_1)\, p_\alpha \hat{b}_\alpha^2 \hat{b}_1^2$$

$$- 4p_\alpha p_\beta \hat{b}_\alpha^2 \hat{b}_\beta^2]$$

and

$$b_1^2 = \hat{b}_i \hat{b}_j \hat{e}_i^{(1)} \hat{e}_j^{(1)},$$

$$b_\alpha^2 = \hat{b}_i \hat{b}_j \hat{e}_i^{(\alpha)} \hat{e}_j^{(\alpha)},$$

$$b_\alpha^2 b_\beta^2 = \hat{b}_i \hat{b}_j \hat{b}_k \hat{b}_\ell \, \hat{e}_i^{(\alpha)} \hat{e}_j^{(\alpha)} \hat{e}_k^{(\beta)} \hat{e}_\ell^{(\beta)}.$$

To evaluate the $\langle T_i \rangle$ values we need a generalisation of equation (74). It can be shown that[23]

$$\hat{e}_i^{(\alpha)} \hat{e}_j^{(\alpha)} = \frac{1}{2} \hat{e}_i^{(1)} \hat{e}_j^{(1)} \, (3\delta_{\alpha 1} - 1) + \frac{1}{2} (\delta_{\alpha 2} + \delta_{\alpha 3}) \delta_{ij}. \qquad (81)$$

The following formulae can then be derived:

$$p_\sigma p_\gamma \langle \hat{e}_\gamma^{(\sigma)} \hat{e}_\gamma^{(\sigma)} \rangle_{\hat{h}} = 3,$$

$$p_\alpha p_\sigma s_\gamma \hat{b}_i \hat{b}_j \langle \hat{e}_i^{(\alpha)} \hat{e}_j^{(\alpha)} \hat{e}_\gamma^{(\sigma)} \hat{e}_\gamma^{(\sigma)} \rangle_{\hat{h}} = 3 + \frac{3}{10} (p_1 - 1)^2 (s_\alpha \hat{b}_\alpha^2 - 1),$$

$$p_\alpha^2 p_\sigma s_\gamma \hat{b}_i \hat{b}_j \langle \hat{e}_i^{(\alpha)} \hat{e}_j^{(\alpha)} \hat{e}_\gamma^{(\sigma)} \hat{e}_\gamma^{(\sigma)} \rangle_{\hat{h}} = p_\alpha p_\alpha + \frac{1}{10} (3p_1^2 - p_\alpha p_\alpha)(p_1 - 1)(s_\alpha \hat{b}_\alpha^2 - 1),$$

$$p_\sigma s_\gamma \hat{b}_i \hat{b}_j \langle \hat{e}_i^{(1)} \hat{e}_j^{(1)} \hat{e}_\gamma^{(\sigma)} \hat{e}_\gamma^{(\sigma)} \rangle_{\hat{h}} = 1 + \frac{1}{5} (p_1 - 1)(s_\alpha \hat{b}_\alpha^2 - 1),$$

$$p_\alpha p_\sigma s_\gamma \hat{b}_i \hat{b}_j \hat{b}_k \hat{b}_\ell \langle \hat{e}_i^{(1)} \hat{e}_j^{(1)} \hat{e}_k^{(\alpha)} \hat{e}_\ell^{(\alpha)} \hat{e}_\gamma^{(\sigma)} \hat{e}_\gamma^{(\sigma)} \rangle_{\hat{h}} = \frac{1}{5} (2p_1 + 3)$$

$$+ \frac{1}{70} (11p_1 + 3)(p_1 - 1)(s_\alpha \hat{b}_\alpha^2 - 1),$$

$$p_\alpha^2 p_\sigma s_\gamma \hat{b}_i \hat{b}_j \hat{b}_k \hat{b}_\ell \langle \hat{e}_i^{(1)} \hat{e}_j^{(1)} \hat{e}_k^{(\alpha)} \hat{e}_\ell^{(\alpha)} \hat{e}_\gamma^{(\sigma)} \hat{e}_\gamma^{(\sigma)} \rangle_{\hat{h}} = \frac{1}{5} (2p_1^2 + p_\alpha p_\alpha)$$

$$+ \frac{1}{70} (11p_1^2 + p_\alpha p_\alpha)(p_1 - 1)(s_\alpha \hat{b}_\alpha^2 - 1),$$

$$p_\alpha p_\beta p_\sigma s_\gamma \hat{b}_i \hat{b}_j \hat{b}_k \hat{b}_\ell \langle \hat{e}_i^{(\alpha)} \hat{e}_j^{(\alpha)} \hat{e}_k^{(\beta)} \hat{e}_\ell^{(\beta)} \hat{e}_\gamma^{(\sigma)} \hat{e}_\gamma^{(\sigma)} \rangle_{\hat{h}} = \frac{1}{5} (3p_1^2 - 6p_1 + 18)$$

$$+ \frac{1}{35} (3p_1^2 + 15p_1 - 18)$$

$$\cdot (p_1 - 1)(s_\alpha \hat{b}_\alpha^2 - 1).$$

Using these and equation (62), $\langle E_s^e (E_s^i)^2 \rangle$ can be evaluated according to equations (79) and (80). The result is:

$$\langle E_s^e (E_s^i)^2 \rangle = \frac{P^3 Q^2 k_o^2 \varepsilon}{r^6} [C^o + D^o (1 - p_1)(s_\alpha \hat{b}_\alpha^2 - 1)] \qquad (82)$$

where C and D values are given by:

$$C^o = C_1^o p_\alpha p_\alpha + C_2^o p_1^2 + C_3^o p_1 + C_4^o,$$

$$D^o = D_1^o p_\alpha p_\alpha + D_2^o p_1^2 + D_3^o p_1 + D_4^o,$$

and

$$C_1^o = (-7320 + 2640\nu - 7128\nu^2)/5775,$$

$$C_2^o = (-43380 + 3168\nu - 7020\nu^2)/5775,$$

$$C_3^o = (17592 + 67584\nu - 13728\nu^2)/5775,$$

$$C_4^o = (29268 - 4752\nu - 30888\nu^2)/5775,$$

$$D_1^o = (-2100 + 1056\nu + 7128\nu^2)/40425,$$

$$D_2^o = (54024 - 15576\nu - 27192\nu^2)/40425,$$

$$D_3^o = -33798 + 374484\nu + 59136\nu^2)/40425,$$

$$D_4^o = (-31482 + 137808\nu - 73656\nu^2)/40425.$$

For a pure hydrostatic applied stress, i.e. $s_\alpha = 1$,

$$\langle E_s^e (E_s^i)^2 \rangle \Big|_{s_\alpha=1} = \epsilon P \frac{P^2 Q^2 k_o^2}{r^6} C$$

$$= 3\langle E_s^e \rangle \langle (E_s^i)^2 \rangle \tag{83}$$

if we assume that $p_2^2 + p_3^2 = 2p_2p_3$, so that

$$2p_\alpha p_\alpha = 3p_1^2 - 6p_1 + 9$$

is used for both equations (82) and (34a). This verifies that equation (82) has the correct limit.

6.3 CALCULATION OF $d(\beta\bar{E}_s)/d\epsilon$

Using equations (68), (76) and (82) and noting equations (77) and (83), the derivative of $\bar{E}_s$ with respect to ϵ can be evaluated. The first line of equation (68) vanishes, the second line is completely cancelled by the $s_\alpha=1$ components of the third line (note equations (77) and (83)) except $\langle E_s^e \rangle$. Thus,

$$\frac{d(\beta\bar{E}_s)}{d\epsilon}\Big|_{\epsilon=0} = -3\beta P + \beta P(1-p_1)(s_\alpha \hat{b}_\alpha^2 - 1)$$

$$\cdot \left\{ -\frac{3\beta k_o PQ}{r^3}\left[\frac{4}{25}(1-2\nu) + \frac{20-28\nu}{175}(1-p_1)\right] \right. \tag{84}$$

$$\left. + \frac{\beta^2 k_o^2 P^2 Q^2}{r^6} - (H_1 p_\alpha p_\alpha + H_2 p_1^2 + H_3 p_1 + H_4) \right\}$$

where

$$H_1 = (-31500 + 15840\nu + 106920\nu^2)/404250,$$

$$H_2 = (921240 - 277992\nu - 563112\nu^2)/404250,$$

$$H_3 = (-883962 + 5861196\nu + 1507968\nu^2)/404250,$$

$$H_4 = (-206118 + 1867536\nu - 1570536\nu^2)/404250.$$

Separating the isotropic and deviatoric contributions, we can write

$$\left.\frac{d(\beta\bar{E}_s)}{d\varepsilon}\right|_{\varepsilon=0} = \left[\frac{d(\beta\bar{E}_s)}{d\varepsilon}\right]_{iso} + \left[\frac{d(\beta\bar{E}_s)}{d\varepsilon}\right]_{dev} \tag{85}$$

where

$$\left[\frac{d(\beta\bar{E}_s)}{d\varepsilon}\right]_{iso} = -3\beta P + \beta P(1-p_1)\left\{\frac{3\beta k_o PQ}{175r^3}[48 - 84\nu - (20-28\nu)p_1] - \frac{\beta^2 k_o{}^2 P^2 Q^2}{r^6}(H_1 p_\alpha p_\alpha + H_2 p_1{}^2 + H_3 p_1 + H_4)\right\} \tag{86}$$

and

$$\left[\frac{d(\beta\bar{E}_s)}{d\varepsilon}\right]_{dev} = \beta P(1-p_1)\left\{-\frac{3\beta k_o PQ}{175r^3}[48 - 84\nu - (20-28\nu)p_1] + \frac{\beta^2 k_o{}^2 P^2 Q^2}{r^6}(H_1 p_\alpha p_\alpha + H_2 p_1{}^2 + H_3 p_1 + H_4)\right\} s_\alpha \cos^2\phi_\alpha. \tag{87}$$

Here ϕ_α is the angle between the Burgers vector and the αth principal axis of the external stress. The corresponding reaction radii in the presence of a uniform external stress can be written as

$$R_a(\varepsilon_{k\ell}) = R_a(0)\left\{1 + \left[\frac{\Delta R_a}{R_a}\right]_{iso} + \left[\frac{\Delta R_a}{R_a}\right]_{dev}\right\} \tag{88}$$

where the isotropic and deviatoric components of $\Delta R_a/R_a$ are calculated from equations (64) or (65), with the appropriate contribution to $d(\beta\bar{E}_s)/d\varepsilon$ given by equations (86) and (87).

The isotropic component arises from the point-defect size effect interacting with the strain field of the external stress, plus the shape effect interacting with the combined strain fields of the IEDL and the isotropic component of the external stress. It is independent of the stress orientation with respect to the Burgers vector, and is therefore of no interest to us here. The deviatoric component, on the other hand, arises from the shape effect interacting with the combined strain fields of the IEDL and the deviatoric component of the external stress. It depends on the relative orientation of the Burgers vector with respect to the external stress direction, and therefore causes preferred absorption of point defects.

Assuming $\nu = \frac{1}{3}$, and writing

$$\varepsilon = \frac{1}{8\mu}\frac{\mathrm{Tr}\sigma_{k\ell}}{3} \equiv \frac{1}{8}\frac{\sigma}{3\mu} \tag{89}$$

where μ is the shear modulus and $\sigma_{k\ell}$ is the applied stress, we can write

$$\left[\frac{\Delta R_a}{R_a}\right]_{dev} = -\frac{1}{8}\beta P \frac{\sigma}{\mu}\mathscr{A} s_\alpha \cos^2\phi_\alpha \tag{90}$$

where $\mathscr{A}$ is the point-defect shape factor given by

$$\begin{aligned}\mathscr{A} = {} & \frac{\mathrm{sign}\,(PQ)}{175}(1-p_1)\,[48-84\nu-(20-28\nu)p_1]\,G_5(A,B)/S(A,B) \\ & + \frac{1}{3}(1-p_1)(H_1 p_\alpha p_\alpha + H_2 p_1^{\,2} + H_3 p_1 + H_4)\,G_8(A,B)/S(A,B)\end{aligned} \tag{91}$$

where $G_n(A,B)$ is defined similar to $S(A,B)$ in equation (50), with t^{-2} replaced by t^{-n}. We note that $\mathscr{A}$, and hence $[\Delta R_a/R_a]_{dev}$, vanish for an isotropic saddle-point configuration ($p_1 = 1$).

It is interesting to compare this result with the corresponding stress-induced change of the reaction radius due to the usual SIPA effect. The expression $(\Delta R_a/R_a)^{SIPA}_{dev}$ has been worked out for a straight edge dislocation, and depends both on the line direction and the Burgers vector direction[20]. If we assume that a dislocation loop may be approximated by averaging the line direction of an edge dislocation in a plane to which the Burgers vector is normal, we obtain

$$\left[\frac{\Delta R_a}{R_a}\right]^{SIPA}_{dev} = - Z_o \frac{\sigma}{\mu} \frac{1}{\varepsilon_o} \Delta W \, s_\alpha \cos^2\phi_\alpha \qquad (92)$$

where ΔW is given by

$$\Delta W = \frac{5}{6} \frac{5\Delta\mu}{30(1-\nu) - 4(4-5\nu)\Delta\mu} . \qquad (93)$$

We have used the average[22]

$$\overline{\cos^2\lambda_n} = \frac{1}{2} (1-\cos^2\phi_\alpha) \qquad (94)$$

and note that $s_\alpha = (3,0,0)$ for a uniaxial stress. Here $\mu(1 + \Delta\mu)$ is the shear modulus of the point defect at the saddle-point configuration, and λ_n is the angle between the line direction and the nth principal direction of the stress.

Comparing equations (90) and (92), we find that the stress dependence and the orientation dependence are identical in the two cases. As we shall see later on, if the point defect is soft in shear at the saddle-point configuration ($\Delta W = - 0.39$ for $\Delta\mu = - 1$, and $- 0.136$ for $\Delta\mu = - 0.5$), the magnitude of SAPSE is several times that of SIPA, for the temperature range in which irradiation creep is important. Also, similar to the usual SIPA in equation (90), equation (92) predicts that the application of the external stress affects the migration of vacancies and interstitials to the loops to a different extent, according to the orientation of the Burgers vector, thereby increasing the bias of

some loops, and decreasing the bias of others that are differently oriented. Thus, the saddle-point shape effect (SAPSE) is also effective in causing a stress-induced preferred absorption, as is the usual SIPA mechanism.

Despite the similarities of the two mechanisms, we must remember that the origins of these two mechanisms are quite different. SAPSE is caused by the interaction of the applied stress with the intrinsic anisotropy of the point-defect configuration at the saddle point. On the other hand, SIPA is caused by the interaction of the applied stress with the induced (by external stress) anisotropy of the point-defect configuration at the saddle point. When the intrinsic anisotropy of the point-defect shape at the saddle point is small and the elastic polarizability of the point defect at the saddle point is large, SIPA dominates over SAPSE. Otherwise, we expect the opposite. At this point, we note that a classical example used for SIPA is the split dumbbell interstitial[19], which deforms significantly under the action of a shear stress. However, one must be careful that, while there is ample evidence in many materials that the interstitial configuration at the equilibrium position is consistent with the split-dumbbell picture, it is not obvious that this can be generalized to the saddle-point configuration.

Although SIPA and SAPSE are indistinguishable as far as the linear stress dependence and stress-orientation dependence of the irradiation creep rate are concerned, these two mechanisms do differ in other aspects. The first important difference arises from the dependence of SAPSE on sign (Q). This behaviour differs from that of SIPA, where the external applied stress has the same effect on both types of loops. Physically, this dependence of the stress effect on sign (Q), i.e. the loop nature, can be understood as follows. Let us first consider the $P > 0$ case. We again refer to Figures 2 and 3. Here the defect enters the dislocation loop through the dilatational region. The application of a uniaxial tensile stress in the direction of $\hat{p}$ enhances the anisotropy of the loop strain field in the dilatational region. In

Section 5, we described how this anisotropy causes the M-type defects to enter the vacancy loop at a faster rate than the F-type defects. The enhancement of this anisotropy by an external stress would enlarge the difference between the currents of the two types of defects. Based on the same argument, the effect on the interstitial loops is opposite, namely, the increase in the reaction radius will be larger for the F-type loops than for the M-type loops. When the external stress is applied in a direction perpendicular to $\hat{b}$, the anisotropy of the loop field will be reduced and the stress will have the opposite effect. For defects with $P < 0$, we must notice that they enter the loop through the compressive region. Application of the foregoing argument shows that the stress effect is opposite to the $P > 0$ case, consistent with the dictates of equation (90).

The second difference between SIPA and SAPSE is the temperature dependence. SAPSE is inversely proportional to the absolute temperature explicitly, while SIPA is not explicitly temperature dependent. However, in an actual experiment, it is not so easy to isolate the temperature dependence of other effects, such as thermal emission of vacancies from sinks, or bulk recombination.

The third difference is the dependence on the point-defect size. SAPSE is directly proportional to the point-defect size, through $|P|$, while SIPA is inversely proportional to the point-defect size. These differences may allow experimental differentiation of SIPA and SAPSE.

7. APPLICATION TO FCC COPPER

We now apply the theory developed in the foregoing sections to study the case of fcc copper. In this case the saddle-point dipole tensors of the vacancy and interstitial have been calculated by computer simulation[6] (see Table 1).

Using equation (90), we may rewrite equation (66) as

$$\Delta B_{jL} = \Delta T_{jL}(1-B_{jL}) \frac{\sigma}{\mu} s_\alpha \cos^2\phi_\alpha \qquad (95)$$

where

$$\Delta T_{jL} = -\frac{1}{8} \beta(P_i \mathcal{A}_i^{jL} - P_v \mathcal{A}_v^{jL}) \qquad j = i,v. \qquad (96)$$

If we assume that $Z_o/\varepsilon_o \simeq 1$, and the vacancy is hard in shear, as usual, then the comparison of ΔT_{jL} with $-\Delta W$ in equation (93) for the interstitials would give us an estimate of the significance of SAPSE as measured against SIPA.

In Table 2, we list the results for the biases, B_{iL} and B_{vL}, for the interstitial loop and the vacancy loop, respectively. Values for ΔT_{iL} and ΔT_{vL} are also calculated and compared with $-\Delta W$. The dipole tensors corresponding to two interatomic potentials of the modified Morse type[6] have been used. The results corresponding to the two potentials show satisfactory consistency. The vacancy loops are seen to have a significantly higher bias for interstitials than the interstitial loops. This can be expected from the discussion in Section 5, because the vacancies in this case are F-type defects and the interstitials are M-type defects (see Table 1). This result is consistent with the fact that void growth, rather than vacancy loop growth, occurs in copper[15]. In fact, a vacancy loop in this case will absorb more interstitials than vacancies and start to shrink the moment it is created from cascade collapse. In effect, the vacancy loops only act as recombination centres. The void swelling behaviour of this material should be well described by theories that include the effect of vacancy-loop creation and shrinkage (see e.g. Bullough, Eyre and Kristian[24]).

The effect of an externally applied stress to the bias can be seen from the results for ΔT_{iL} and ΔT_{vL}. From these, it can be deduced from equation (90) that the application of a uniaxial tensile stress in

the direction of $\hat{b}$ increases the biases of both types of loops. The increase is bigger for vacancy loops than for interstitial loops. As we have discussed in Section 6, this result can be understood immediately from Figures 2 and 3. In the present case, both P_i and P_v are positive, and hence both defects enter the dislocation loop from the dilatational region. The effect of the stress is to increase the anisotropy of the loop in these regions. Since the stress-free bias difference between the B_{iL} and B_{vL} is due to this anisotropy in the first place, its enhancement by the external stress further increases the difference between B_{iL} and B_{vL}. The application of a uniaxial compressive stress along the direction of $\hat{b}$ would reduce the stress-free bias differential between B_{iL} and B_{vL}. From this discussion, the application of a stress in copper would produce a SAPSE effect assisting the SIPA effect. At this point, we should point out that the foregoing discussion is appropriate for small loops only; it may not be applicable to a straight-edge dislocation, or a large loop, where results are not available at present.

To estimate the significance of SAPSE, we compare the values of ΔT_{iL} and ΔT_{vL} with $-\Delta W$ at a typical temperature of 500 K for irradiation damage experiments. Two values of $\Delta\mu$ are taken, $\Delta\mu = -1$, corresponding to a zero shear modulus of the defect, and $\Delta\mu = -0.5$, corresponding to a 50% reduction of the shear modulus near the defect. It can be seen (Table 2) that the magnitude of the ΔT values are much bigger than ΔW showing that the SAPSE effect may be significant and is worthy of consideration when studying irradiation creep.

8. SUMMARY AND CONCLUSIONS

Point-defect migration into an infinitesimal edge dislocation loop in an isotropic linear elastic medium has been studied. Particular care was taken to include the effects of the saddle-point shape anisotropy of the point defect. Expressions for the reaction radii and the

bias have been derived, both in the presence and absence of an external applied stress. The expressions were found to depend on intrinsic parameters, such as the loop strength, the loop nature (vacancy or interstitial), the relaxation volumes, the shapes at the saddle point, and also extrinsic parameters, such as the magnitude and direction of the external stress, and the temperature. From these expressions, the following general conclusions can be drawn:

1. For point defects with an anisotropic shape at the saddle point, there is an intrinsic difference between the reaction radii of a vacancy loop and an interstitial loop. In this context, point defects can be divided into M-type (elongated in the jump direction), F-type (elongated in the plane normal to the jump direction), and N-type (isotropic), according to their saddle-point configurations. The vacancy loops have the largest reaction radii for M-type defects and the smallest for F-type defects. The opposite is true for interstitial loops. This causes an intrinsic bias differential between vacancy loops and interstitial loops.

2. Depending on the relative strengths of the size effect and the shape effect, it is not inconceivable that vacancy loops or interstitial loops with a negative bias (i.e. a preference for vacancies) exist in some materials.

3. The application of an external stress changes the bias of a dislocation loop in a way somewhat similar to the usual SIPA. However, the magnitude of the change is much bigger. It also increases linearly with σ/μ and varies similarly with the stress orientation. However, there are important differences also. Firstly, the change depends on the loop nature. Secondly, the magnitude of the change is explicitly proportional to T^{-1}, and thirdly, the magnitude of the change is directly, rather than inversely, proportional to the point-defect size.

ACKNOWLEDGEMENTS

The author would like to thank Dr. R. Dutton for a critical reading of the manuscript and for his many useful suggestions. Stimulating discussions with Drs. G.V. Kidson and I.G. Ritchie are also gratefully acknowledged.

REFERENCES

1. H. Ullmaier and W. Schilling, "Radiation Damage in Metallic Reactor Materials", IN Physics of Modern Materials, p. 301, International Atomic Energy Agency, Vienna (1980).

2. R. Bullough and R.C. Perrin, "Growth Stability and Interactions of Voids and Gas Bubbles in Solids", IN Proceedings of Symposium Radiation Damage in Reactor Materials, IAEA 2, 233, Vienna (1969).

3. P.H. Dederichs and K. Schroeder, "Anisotropic Diffusion in Stress Fields", Phys. Rev. B 17, 2524 (1978).

4. W.G. Wolfer and M.Ashkin, "Stress Induced Diffusion of Point Defects to Spherical Sinks", J. Appl. Phys. 46, 547 (1975).

5. K. Schroeder and K. Dettmann, "Diffusion Reactions in Long Range Potentials", Z. Phys. B 22, 343 (1975).

6. P.H. Dederichs, C. Lehmann, H.R. Schober, A Scholz and R. Zeller, "Lattice Theory of Point Defects", J. Nucl. Mat. 69&70, 176 (1978).

7. K. Ong, C.H. Woo and J. Vail, unpublished results.

8. R. Bullough, D.W. Wells, J.R. Wilks and M.H. Wood, Acta Met., in press.

9. W.A. Coghlan, "Transient and Steady State Diffusion Solution for Point Defects in a Stress Field", IN Proceedings of Conference on Computer Simulation for Materials Applications, (National Bureau of Standards, Gaithersburg, MD (1976)), Nuclear Metallurgy 20, Part 1, p. 166.

10. M.H. Yoo and W.H. Butler, "Steady-State Diffusion of Point Defects in the Interaction Force Field", Phys. Status Solidi B 77(1), 181 (1976).

11. C.H. Woo, "The Sink Strength of a Dislocation Loop in the Effective Medium Approximation", J. Nucl. Mat. 98, 279 (1981).

12. See for example, A.D. Brailsford, R. Bullough and M.R. Hayns, "Point Defect Sink Strengths and Void-Swelling", J. Nucl. Mater. 60, 246 (1976), or reference (11).

13. F. Kroupa, "Dislocation Loops", IN Theory of Crystal Defects, Proceedings of the Summer School, Hrazany, September 1964, Ed. Boris Gruber, Academic Press, New York and London (1966) p. 275.

14. R. Bullough, J.T. Stanley and J.M. Williams, "The Kinetics of Migration of Impurities to Small Dislocation Loops", Metal Science Journal 2, 93 (1968).

15. J.O. Stiegler, "Void Formation in Neutron-Irradiated Metals", IN Radiation-Induced Voids in Metals, Proceedings of the 1971 International Conference at Albany, New York, Eds. J.W. Corbett and L.C. Ianniello, U.S. Atomic Energy Commission, Office of Information Services (1972), p. 292.

16. D. Faulkner and C.H. Woo, "Void Swelling in Zirconium", J. Nucl. Mater. 90, 307 (1980).

17. P.T. Heald and M.V. Speight, "Steady State Irradiation Creep", Philos. Mag. 29, 1075 (1974).

18. W.G. Wolfer and M. Ashkin, "Diffusion of Vacancies and Interstitials to Edge Dislocations", J. Appl. Phys. 47, 791 (1976).

19. R. Bullough and J.R. Willis, "The Stress-Induced Point Defect-Dislocation Interaction and Its Relevance to Irradiation Creep", Philos. Mag. 31, 855 (1975).

20. C.H. Woo, "Effects of an Anisotropic Dislocation Structure on Irradiation Creep Due to Stress Induced Preferred Absorption of Point Defects", J. Nucl. Mater. 80, 132 (1979).

21. C.H. Woo, "Irradiation Creep Due to Climb-Induced Glide in an Anisotropic Dislocation Structure", J. Nucl. Mater. 98 (1981) in press.

22. E.J. Savino, "Point Defect-Dislocation Interaction in a Crystal Under Tension", Philos. Mag. 36, 323 (1977).

23. B.L. Skinner, private communication.

24. R. Bullough, B.L. Eyre and K. Krishan, "Cascade Damage Effects on the Swelling of Irradiated Materials", Proc. Roy. Soc. (London), A346, 81 (1975).

25. H. Goldstein, "Classical Mechanics", Addison-Wesley, Cambridge, Mass. (1950).

TABLE 1

PARAMETERS FOR VACANCIES AND INTERSTITIALS IN THE SADDLE-POINT CONFIGURATION FOR f.c.c. COPPER, OBTAINED BY COMPUTER SIMULATION[6]

Defect	Potentials	TrP(eV)	p_1	p_2	p_3	$\hat{e}^{(1)}$ (= $\hat{h}$)	$\hat{e}^{(2)}$	$\hat{e}^{(3)}$	Defect Type (M or F)
Vacancy Migration	M0	5.61	-0.73	0.21	3.52	$\begin{pmatrix}1\\1\\0\end{pmatrix}$	$\begin{pmatrix}1\\-1\\0\end{pmatrix}$	$\begin{pmatrix}0\\0\\1\end{pmatrix}$	F
<100> Interstitial Migration	M0	68.9	1.10	0.87	1.03	$\begin{pmatrix}1\\0\\1\end{pmatrix}$	$\begin{pmatrix}1\\0\\-1\end{pmatrix}$	$\begin{pmatrix}0\\1\\0\end{pmatrix}$	M
Vacancy Migration	M1	3.4	-1.13	0	4.13	$\begin{pmatrix}1\\1\\0\end{pmatrix}$	$\begin{pmatrix}1\\-1\\0\end{pmatrix}$	$\begin{pmatrix}0\\0\\1\end{pmatrix}$	F
<100> Interstitial Migration	M1	45.6	1.14	0.83	1.03	$\begin{pmatrix}1\\0\\1\end{pmatrix}$	$\begin{pmatrix}1\\-1\\0\end{pmatrix}$	$\begin{pmatrix}0\\0\\1\end{pmatrix}$	M

TABLE 2

RESULTS FOR THE BIASES AND THE EFFECT OF STRESS ON THE BIASES OF VACANCY AND INTERSTITIAL LOOPS IN COPPER

(See text for meaning of symbols)

Interatomic Potential	B_{vL}	B_{iL}	ΔT_{vL} (500 K)	ΔT_{iL} (500 K)	$-\Delta W$ ($\Delta\mu = -1$)	ΔW ($\Delta\mu_i = -0.5$)
M0	0.527	0.327	1.029	0.789	0.39	0.136
M1	0.498	0.294	0.944	0.795	0.39	0.136

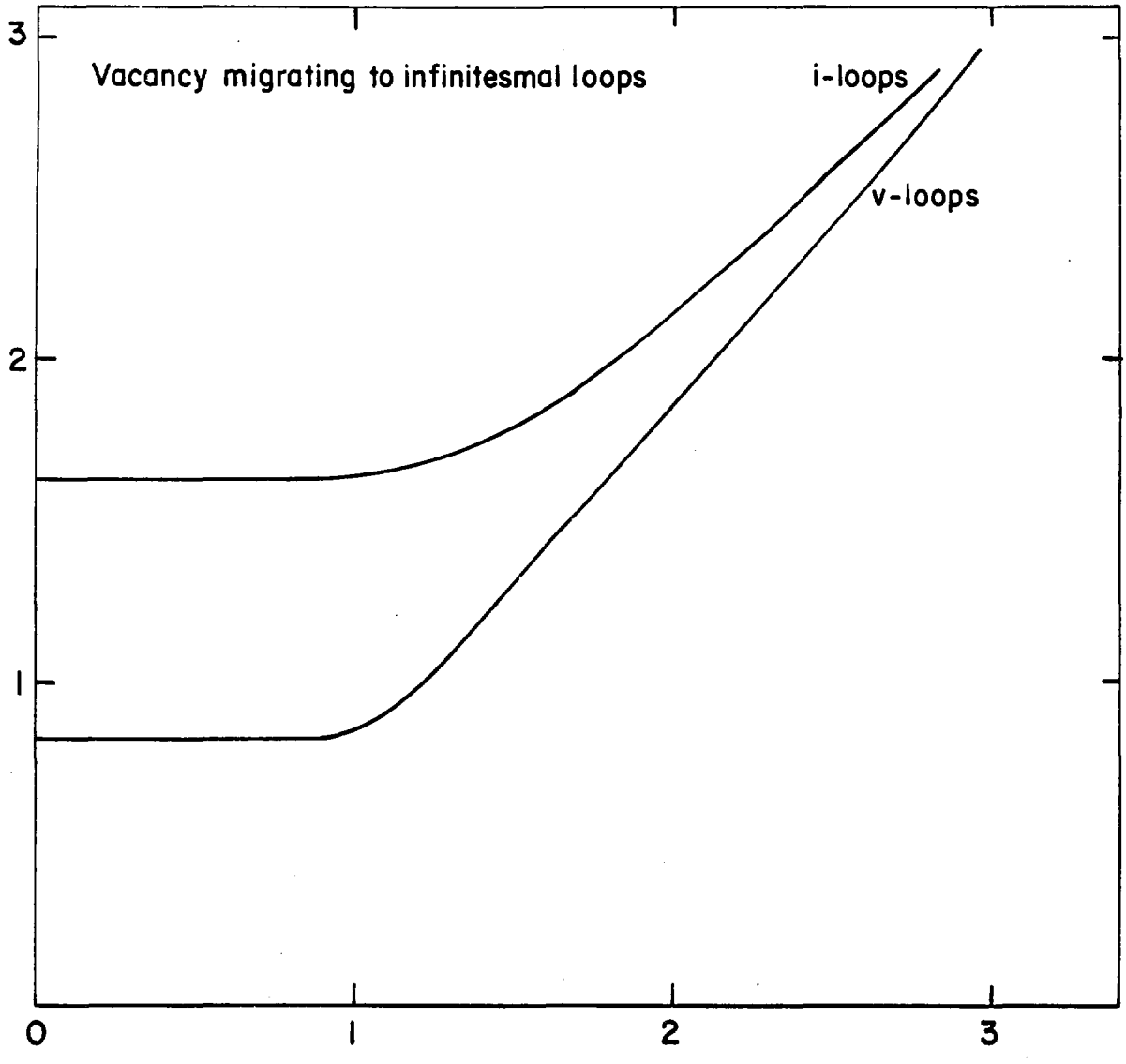

FIGURE 1: Variation of $|k_o \beta PQ|^{-1/3} R_a$ with t_σ (see equation (40a)). Note the insensitivity of R_a when $t_\sigma < 1$.

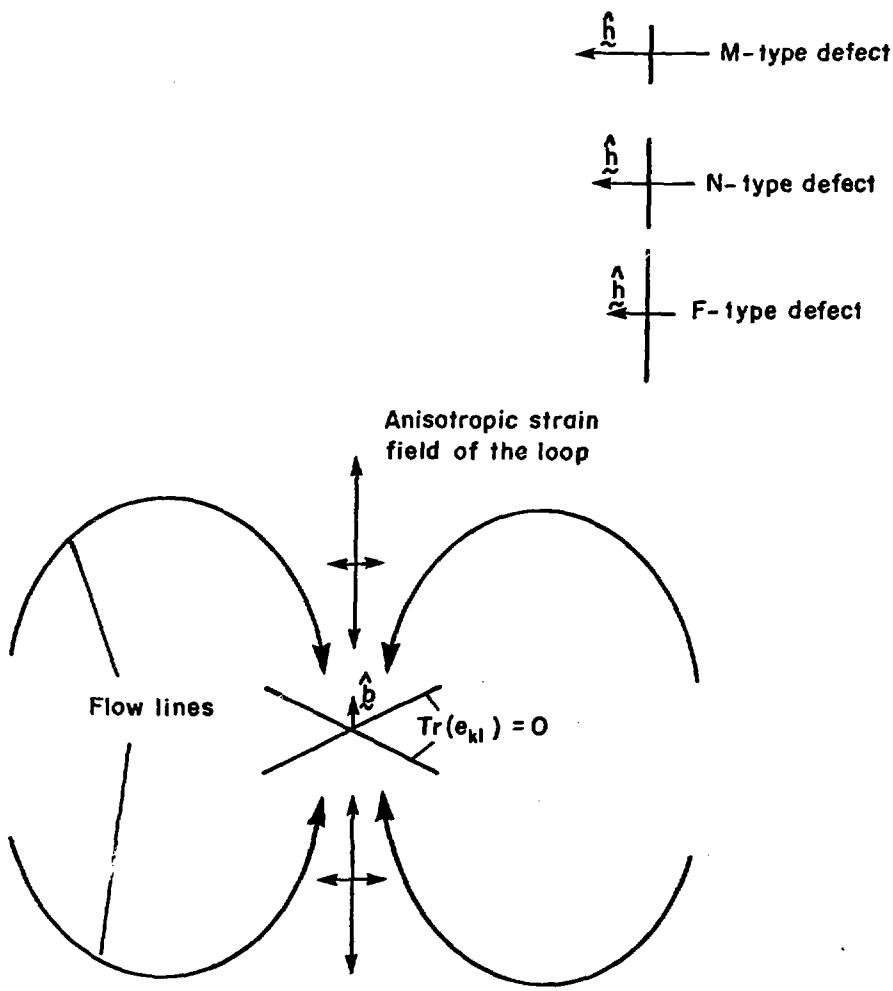

FIGURE 2: Point-Defect (with P > 0) Migration to a Vacancy Dislocation Loop, Showing the Flow Lines and the Anisotropy of the Loop Strain Field. Also shown are the dipole expansion fields of the three types of defects, M, N, and F. Note the good "fit" of the M-type defects into the anisotropic strain field of the loop during the jump in the direction of the flow lines, as compared to the bad "fit" of the F-type defects.

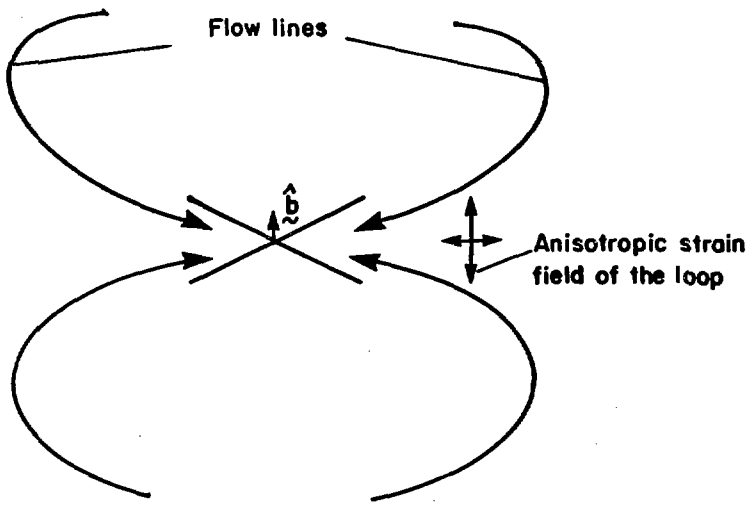

FIGURE 3: Point-Defect (with P > 0) Migration to an Interstitial Dislocation Loop, Showing the Flow Lines and the Anisotropy of the Loop Strain Field.

APPENDIX A

In this appendix, we show that

$$\beta\bar{E}_s(r) = 3\langle\beta E_s\rangle - \frac{3}{2}\langle\beta^2 E_s{}^2\rangle + \frac{9}{2}\langle\beta E_s\rangle^2 + O(r^{-9}). \qquad \text{(A-1)}$$

Let us define $a \equiv 1/\langle 1\rangle$.

Then we can write, by expanding $\exp(-\beta E_s)$,

$$\langle\exp(-\beta E_s)\rangle = \langle 1\rangle - \langle\beta E_s\rangle + \frac{1}{2!}\langle\beta^2 E_s{}^2\rangle + \ldots. \qquad \text{(A-2)}$$

and we can calculate the difference, Δ, where

$$\Delta = \exp(-a\langle\beta E_s\rangle + \frac{a}{2}\langle\beta^2 E_s{}^2\rangle - \frac{a^2}{2}\langle\beta E_s\rangle^2) - a\langle\exp(-\beta E_s)\rangle. \qquad \text{(A-3)}$$

Expanding the right-hand side of equation (A-3) in an infinite series, we obtain

$$\Delta = \frac{1}{3!}(2a^3\langle\beta E_s\rangle^3 + a\langle\beta^3 E_s{}^3\rangle - 3a^2\langle\beta E_s\rangle\langle\beta^2 E_s{}^2\rangle)$$

$$- \frac{1}{4!}(2a^4\langle\beta E_s\rangle^4 + a\langle\beta^4 E_s{}^4\rangle - 3a^2\langle\beta^2 E_s{}^2\rangle^2) \qquad \text{(A-4)}$$

$$= O(r^{-9})$$

because $\beta E_s = O(r^{-3})$. Thus, we can write

$$\langle\exp(-\beta E_s)\rangle = \frac{1}{a}\exp(-a\langle\beta E_s\rangle + \frac{a}{2}\langle\beta^2 E_s{}^2\rangle - \frac{a^2}{2}\langle\beta E_s\rangle^2) + O(r^{-9}). \qquad \text{(A-5)}$$

In the present case $\langle 1\rangle = \langle\langle(\hat{r}\cdot\hat{h})^2\rangle_{\hat{r}}\rangle_{\hat{h}} = 1/3$. Using the definition in equation (11), it is straightforward to show that equation (A-1) is true.

APPENDIX B

In this appendix, we discuss the evaluation of the angular integrals

$$\gamma(i_1,i_2\ldots i_n) = \frac{1}{4\mu}\int \hat{r}_{i_1}\hat{r}_{i_2}\ldots\hat{r}_{i_n}\,d\Omega \qquad \text{(B-1)}$$

where $\hat{r}_{i_\mu}$ is the i_μth component of the unit vector $\hat{\underset{\sim}{r}}$ and $d\Omega$ is the elemental solid angle subtended by $d\hat{\underset{\sim}{r}}$. By reflection symmetry across the xy, yz, and zx planes, we conclude that the $\hat{r}_{i_\mu}$ values on the right-hand side of equation (B-1) have to occur in pairs, in order that the integral is non-zero. For example, reflection symmetry across the xy plane requires that the integral be invariant when all $\hat{r}_3$ values are replaced by $-\hat{r}_3$ values. This immediately shows that, for γ to be non-zero, the integrand must contain an even number of $\hat{r}_3$ values.

It is convenient to describe $(i_1,\ldots,i_n)$ as an n-dimensional vector $\underset{\sim}{i}$ and introduce a permutation operator P that permutes the components of $\underset{\sim}{i}$. We also define a pairing operator, Δ, by

$$\Delta(\underset{\sim}{j}) \equiv \Delta(j_1\ldots j_n) \equiv \delta_{j_1j_2}\delta_{j_3j_4}\ldots\delta_{j_{n-1}j_n}. \qquad \text{(B-2)}$$

Using Δ and P, the statement that $\gamma(\underset{\sim}{i})$ is non-zero if (note that the sufficient condition follows from equation (B-6)), and only if the i_μ values occur in pairs can be restated as follows:

$$\gamma(\underset{\sim}{i}) = 0 \quad \text{if and only if } \Delta P(\underset{\sim}{i}) = 0 \quad \text{for every P.} \qquad \text{(B-3)}$$

Since $\Delta P(\underset{\sim}{i})$ is positive definite, statement (B-3) is equivalent to

$$\gamma(\underset{\sim}{i}) = 0 \quad \text{if, and only if, } \sum_P \Delta P(\underset{\sim}{i}) = 0. \qquad \text{(B-4)}$$

Now we notice that in equation (B-2) the right-hand side does not change with the interchange of j_n and j_{n+1} (when n is odd), or with the inter-

change of any two δ values. Thus, even if the i_μ values are all unequal there are $2^{n/2}$ $(n/2)!$ equivalent permutations of the i_μ values that correspond to the same set of δ values on the right-hand side of equation (B-4). Taking this into account, we may rewrite statement (B-4) as

$$\gamma(\underset{\sim}{i}) = C \sum_{P'} \Delta P'(\underset{\sim}{i}) \tag{B-5}$$

where P' is restricted to run over inequivalent permutations (when all i_μ values are considered unequal) only, and C is to be determined in the following.

Suppose $\underset{\sim}{i}$ is made up of n_x pairs of 1 values, n_y pairs of 2 values and n_z pairs of 3 values, then $\gamma(\underset{\sim}{i})$ can be calculated from equation (B-1), viz.,

$$\gamma(\underset{\sim}{i}) = \frac{1}{4\mu} \int_0^{\pi} \cos^{2n_z}\theta \sin^{2(n_x+n_y)}\theta d(\cos\theta) \int_0^{2\pi} \sin^{2n_y}\phi \cos^{2n_x}\phi d\phi$$

$$= \left[\frac{n!}{2^{n/2}(n/2)!}\right]^{-1} \frac{(2n_x)!}{2^{n_x} n_x!} \frac{(2n_y)!}{2^{n_y} n_y!} \frac{(2n_z)!}{2^{n_z} n_z!} \frac{1}{n+1}. \tag{B-6}$$

Let us now consider the right-hand side of equation (B-5). Here $\Delta P'(\underset{\sim}{i})$ is either zero or 1, so that

$$\sum_{P'} \Delta P'(\underset{\sim}{i}) = N \tag{B-7}$$

where N is the total number of P' values, such that $\Delta P'(\underset{\sim}{i}) = 1$. In the present case under consideration, the number of 1 values in $\underset{\sim}{i}$ is $2n_x$, the number of 2 values is $2n_y$ and the number of 3 values, $2n_z$. Any P' value such that $\Delta P'(\underset{\sim}{i}) = 1$ must permute $\underset{\sim}{i}$ into the following form:

$$P'(\underset{\sim}{i}) = (j_1, j_2 \ldots j_{2n_x}, k_1, k_2 \ldots k_{2n_y}, \ell_1, \ell_2 \ldots \ell_{2n_z})$$

where $j_1 = j_2 = \ldots = j_{2n_x} = 1$, $k_1 = k_2 = \ldots = k_{2n_y} = 2$, $\ell_1 = \ell_2 = \ldots = \ell_{2n_z} = 3$.

Therefore the total number, N, of P'values satisfying this condition is given by the number of ways the j values can permute, inequivalently, among themselves, times the number of ways the k values can, among themselves, times the number of ways the ℓ values can, among themselves. Therefore

$$N = \frac{(2n_x)!}{2^{n_x} n_x!} \frac{(2n_y)!}{2^{n_y} n_y!} \frac{(2n_z)!}{2^{n_z} n_z!} . \tag{B-8}$$

Equations (B-5), (B-6) and (B-8) determine C, such that

$$C = \frac{2^{n/2}(n/2)!}{(n+1)!} \tag{B-9}$$

which only depends on n and is independent of other details of $\underset{\sim}{i}$. Thus, we have

$$\gamma(\underset{\sim}{i}) = \frac{2^{n/2}(n/2)!}{(n+1)!} \Gamma(\underset{\sim}{i}) \tag{B-10}$$

where

$$\Gamma(\underset{\sim}{i}) = \sum_{P'} \Delta P'(\underset{\sim}{i}) . \tag{B-11}$$

The evaluation of equation (B-10) is quite easy, when n is small. For example, when n = 4

$$\gamma(ijk\ell) = \frac{1}{15} [\Delta(kjk\ell) + \Delta(ikj\ell) + \Delta(i\ell jk)]$$

$$= \frac{1}{15} (\delta_{ij}\delta_{k\ell} + \delta_{ik}\delta_{j\ell} + \delta_{i\ell}\delta_{jk})$$

and

$$\Gamma(ijk\ell) = \delta_{ij}\delta_{k\ell} + \delta_{ik}\delta_{j\ell} + \delta_{i\ell}\delta_{jk} .$$

However, it quickly becomes very cumbersome as n increases. For example, when n = 10, the largest n we encounter in the present paper, there are in

general 945 terms in $\gamma(\underset{\sim}{i})$, each made up of a product of five δ functions. In such a case, we need a formula by which the evaluation of γ may be simplified.

We note that, by fixing i_1 to be in the first pair, we can write, for any P' value,

$$P'(\underset{\sim}{i}) = (i_1, i_\mu, P'(\underset{\sim}{i} - \{i_1, i_\mu\})) \qquad \text{for } \mu = 2,3\ldots n$$

where $(\underset{\sim}{i} - \{i_1, i_\mu\})$ is an (n-2) dimension vector which has all its components equal to those of $\underset{\sim}{i}$ and in the same order, except for i_1 and i_μ, which are excluded. We can then write, for any P' value,

$$\Delta P'(\underset{\sim}{i}) = \delta_{i,i_\mu} \Delta P''(\underset{\sim}{i} - \{i, i_\mu\}) \tag{B-12}$$

and

$$\sum_{P'} \Delta P'(\underset{\sim}{i}) = \sum_{\mu=2}^{n} \delta_{i,i_\mu} \sum_{P''} \Delta P''(\underset{\sim}{i} - \{i, i_\mu\}). \tag{B-13}$$

Thus

$$\Gamma(\underset{\sim}{i}) = \sum_{\mu=2}^{n} \delta_{i,i_\mu} \Gamma(\underset{\sim}{i} - \{i, i_\mu\}). \tag{B-14}$$

Once $\Gamma(\underset{\sim}{i})$ is evaluated, $\gamma(\underset{\sim}{i})$ can be obtained directly from equation (B-10).

Thus, for example

$$\Gamma(ijk\ell mn) = \delta_{ij}\Gamma(k\ell mn) + \delta_{ik}\Gamma(j\ell mn) + \delta_{i\ell}\Gamma(jkmn)$$

$$+ \delta_{im}\Gamma(jk\ell n) + \delta_{in}\Gamma(jk\ell m).$$

In the case when $i_1 = i_2$, we have further simplification:

$$\Gamma(\underset{\sim}{i}) = \sum_{\mu=2}^{n} \delta_{i_1 i_\mu} \Gamma(\underset{\sim}{i} - \{i_1, i_2\})$$

$$= \Gamma(\underset{\sim}{i} - \{i_1, i_2\}) \left(1 + \sum_{\mu=3}^{n} \delta_{i_1, i_\mu}\right). \qquad \text{(B-15)}$$

Here, all terms with $i_\mu \neq i_2$ can be excluded from the sum because the condition $i_1 = i_2$ requires $i_2 = i_\mu$ for δ_{i,i_μ} to be non-zero.

Using equation (B-14) and the special case of equation (B-15), we can evaluate quickly many cases. Thus, a large-n case that has many repeated indices can be readily reduced to a small-n case. For example,

$$\Gamma(\alpha\alpha\beta\beta\gamma\gamma ijk\ell) = (1 + 2\delta_{\alpha\beta} + 2\delta_{\alpha\gamma} + \delta_{\alpha i} + \delta_{\alpha j} + \delta_{\alpha k} + \delta_{\alpha\ell})\ \Gamma(\beta\beta\gamma\gamma ijk\ell)$$

$$= (1 + 2\delta_{\alpha\beta} + 2\delta_{\alpha\gamma} + \delta_{\alpha i} + \delta_{\alpha j} + \delta_{\alpha k} + \delta_{\alpha\ell})$$

$$\cdot\ (1 + 2\delta_{\beta\gamma} + \delta_{\beta i} + \delta_{\beta j} + \delta_{\beta k} + \delta_{\beta\ell})$$

$$\cdot\ (1 + \delta_{\gamma i} + \delta_{\gamma j} + \delta_{\gamma k} + \delta_{\gamma\ell})\ \Gamma(ijk\ell).$$

Furthermore, in many cases i,j,k,ℓ may be equivalent, and further simplification takes place. In this case,

$$\Gamma(\alpha\alpha\beta\beta\gamma\gamma ijk\ell) = (1 + 2\delta_{\alpha\beta} + 2\delta_{\alpha\gamma} + 4\delta_{\alpha i})\ (1 + 2\delta_{\beta\gamma} + 4\delta_{\beta i})$$

$$\cdot\ (1 + 4\delta_{\gamma i})\ \Gamma(ijk\ell).$$

APPENDIX C

Let θ, ϕ and ψ be the three Eulerian angles[25] between the basis sets $\hat{e}^{(\sigma)}$ and $\hat{t}^{(\sigma)}$. In terms of the $\hat{t}^{(\sigma)}$ values, the $\hat{e}^{(\sigma)}$ values can be expressed as the following column vectors

$$\underset{\sim}{\hat{e}}^{(1)} = \begin{pmatrix} \sin\theta\cos\phi \\ \sin\theta\sin\phi \\ \cos\theta \end{pmatrix}, \qquad \underset{\sim}{\hat{e}}^{(2)} = \begin{pmatrix} \sin\phi\cos\psi + \cos\theta\cos\phi\sin\psi \\ -\cos\phi\cos\psi + \cos\theta\sin\phi\sin\psi \\ -\sin\theta\sin\psi \end{pmatrix},$$

$$\underset{\sim}{\hat{e}}^{(3)} = \begin{pmatrix} -\sin\phi\sin\psi + \cos\theta\cos\phi\cos\psi \\ \cos\phi\sin\psi + \cos\theta\sin\phi\cos\psi \\ -\sin\theta\cos\psi \end{pmatrix}.$$

We can now evaluate the squares of each component of $\underset{\sim}{\hat{e}}^{(2)}$ and $\underset{\sim}{\hat{e}}^{(3)}$. For $\underset{\sim}{\hat{e}}^{(2)}$:

$$\hat{e}^{(2)}_\gamma \hat{e}^{(2)}_\gamma \text{ (no implied summation)} = \begin{pmatrix} \sin^2\phi\cos^2\psi + \cos^2\theta\cos^2\phi\sin^2\psi + 2\cos\theta\sin\phi\cos\phi\sin\psi\cos\psi \\ \cos^2\phi\cos^2\psi + \cos^2\theta\sin^2\phi\sin^2\psi - 2\cos\theta\sin\phi\cos\phi\sin\psi\cos\psi \\ \sin^2\theta\sin^2\psi \end{pmatrix}.$$

In the above description, the angle ψ represents a rotation about $\underset{\sim}{\hat{e}}^{(1)}$. For simplicity, we assume that ψ is distributed randomly, so that we may average over ψ and assume $\cos^2\psi = \frac{1}{2} = \sin^2\psi$, $\sin\psi\cos\psi = 0$. Then $\hat{e}^{(2)}_\gamma \hat{e}^{(2)}_\gamma$ becomes

$$\hat{e}^{(2)}_\gamma \hat{e}^{(2)}_\gamma = \frac{1}{2}\begin{pmatrix} \sin^2\phi + \cos^2\theta\cos^2\phi \\ \cos^2\phi + \cos^2\theta\sin^2\phi \\ \sin^2\theta \end{pmatrix} = \frac{1}{2}\left(1 - \hat{e}^{(1)}_\gamma \hat{e}^{(1)}_\gamma\right).$$

Similarly, we can show the same for $\hat{e}^{(3)}_\gamma \hat{e}^{(3)}_\gamma$. Thus, we can write

$$\hat{e}^{(\sigma)}_\gamma \hat{e}^{(\sigma)}_\gamma = \delta_{\sigma 1}\hat{e}^{(1)}_\gamma \hat{e}^{(1)}_\gamma + \frac{1}{2}(1-\delta_{\sigma 1})(1-\hat{e}^{(1)}_\gamma \hat{e}^{(1)}_\gamma)$$

$$\text{(no implied summation)} = \frac{1}{2}\hat{e}^{(1)}_\gamma \hat{e}^{(1)}_\gamma (3\delta_{\sigma 1}-1) + \frac{1}{2}(\delta_{\sigma 2}+\delta_{\sigma 3}).$$

ISSN 0067-0367

To identify individual documents in the series we have assigned an AECL- number to each.

Please refer to the AECL- number when requesting additional copies of this document from

Scientific Document Distribution Office
Atomic Energy of Canada Limited
Chalk River, Ontario, Canada
KOJ 1JO

Price: $4.00 per copy

ISSN 0067-0367

Pour identifier les rapports individuels faisant partie de cette série nous avons assigné un numéro AECL- à chacun.

Veuillez faire mention du numéro AECL -si vous demandez d'autres exemplaires de ce rapport au

Service de Distribution des Documents Officiels
L'Energie Atomique du Canada Limitée
Chalk River, Ontario, Canada
KOJ 1JO

prix: $4.00 par examplaire